



WETMETH 1.0: A new wetland methane model for implementation in Earth system models

Claude-Michel Nzotungicimpaye¹, Andrew H. MacDougall², Joe R. Melton³, Claire C. Treat⁴, Michael Eby⁵, Lance F.W. Lesack^{1, 6}, Kirsten Zickfeld¹

- 5 ¹Department of Geography, Simon Fraser University, Burnaby, BC, Canada
²Climate and Environment, St. Francis Xavier University, Antigonish, NS, Canada
³Climate Research Division, Environment and Climate Change Canada, Victoria, BC, Canada
⁴Alfred Wegener Institute Helmholtz Centre for Polar and Marine Research, Potsdam, Germany
⁵School of Earth and Ocean Sciences, University of Victoria, Victoria, BC, Canada
10 ⁶Department of Biological Sciences, Simon Fraser University, Burnaby, BC, Canada

Correspondence to: Claude-Michel Nzotungicimpaye (cnzotung@sfu.ca)

Abstract. Wetlands are the single largest natural source of methane (CH₄), a powerful greenhouse gas affecting the global climate. In turn, wetland CH₄ emissions are sensitive to changes in climate conditions such as temperature and precipitation
15 shifts. However, biogeochemical processes regulating wetland CH₄ emissions (namely microbial production and oxidation of CH₄) are not routinely included in fully coupled Earth system models that simulate feedbacks between the physical climate, the carbon cycle, and other biogeochemical cycles. This paper introduces a process-based wetland CH₄ model (WETMETH) developed for implementation in Earth system models and currently embedded in an Earth system model of intermediate complexity. Here we: (i) describe the wetland CH₄ model; (ii) evaluate the model performance against available datasets and
20 estimates from the literature; (iii) analyze the model sensitivity to perturbations of poorly constrained parameters. Historical simulations show that WETMETH is capable of reproducing mean annual emissions consistent with present-day estimates across spatial scales. For the 2008-2017 decade the model simulates global mean wetland emissions of 158.6 Tg CH₄ yr⁻¹, of which 33.1 Tg CH₄ yr⁻¹ are from wetlands north of 45°N. WETMETH is highly sensitive to parameters for the microbial oxidation of CH₄, which is the least constrained process in the literature.



25 1 Introduction

Wetlands are vegetated locations that are inundated with water on a permanent, seasonal or recurrent basis (Wheeler, 1999). In the context of this study, wetlands are defined following the latest global CH₄ budget report (Saunio et al., 2020): natural ecosystems with inundated or water-saturated soils where anoxic conditions lead to the production of CH₄. Wetlands across the globe are the single largest natural source of atmospheric CH₄, accounting for approximately a third of total global emissions (Bridgman et al., 2013; Saunio et al., 2016). Estimates of global wetland CH₄ emissions over the past few decades vary between 140 and 210 Tg CH₄ yr⁻¹ (Kirschke et al., 2013). Although there exist different types of wetlands such as bogs, fens, swamps, marshes and floodplains (Aselmann and Crutzen, 1989; Saunio et al., 2016), the release of CH₄ from any wetland results from the balance between two biogeochemical processes (Segers, 1998): the production of CH₄ by anaerobic microbes (namely methanogens) and the oxidation of CH₄ primarily by aerobic microbes (namely methanotrophs).

Both CH₄ production and oxidation in wetlands are sensitive to changes in climate conditions. For instance, soil warming accelerates the microbial activity with a higher response for methanogenic than methanotrophic activity (Bridgman et al., 2013; Dunfield et al., 1993; Segers, 1998). At the landscape or larger scale, increased wet conditions tend to enhance methanogenic activity to the detriment of methanotrophic activity (Duval and Radu, 2018; Helbig et al., 2017; Kim, 2015). In turn, wetland CH₄ emissions can affect the global climate through changes in atmospheric CH₄ levels and associated radiative forcing (Dean et al., 2018; O'Connor et al., 2010). Analyses of ice cores suggest that CH₄ emissions from tropical and northern wetlands contributed significantly to climate changes during past glacial-interglacial transitions (Loulergue et al., 2008; Rhodes et al., 2017).

The interactions between climate conditions and wetland CH₄ emissions translate into a positive feedback loop that has the potential to amplify changes in global mean surface air temperature, which is a major concern for future climates (Dean et al., 2018; O'Connor et al., 2010). Research on feedbacks between the physical climate and biogeochemical cycles is generally conducted with 3-dimensional (3-D) fully coupled Earth system models (ESMs) (Arora et al., 2013). Over the past decade, these ESMs have proven very useful to investigate and inform international climate policies such as the accounting of carbon emissions required to avoid the risk of dangerous climate change (Zickfeld et al., 2009) and achieve the goals of the Paris Agreement (Tokarska and Gillett, 2018). Yet, biogeochemical processes regulating CH₄ emissions in wetlands are not commonly included in fully coupled ESM simulations.

In the past, several process-based models have been developed for investigating the response of wetland CH₄ emissions to climate variability and climate change (Hodson et al., 2011; Hopcroft et al., 2011; Pandey et al., 2017; Paudel et al., 2016; Shindell et al., 2004; Zhang et al., 2018; Zhu et al., 2015). These wetland CH₄ models are generally embedded in terrestrial or land surface models and forced with observational datasets or reanalysis products (Melton et al., 2013; Wania et al., 2013; Xu et al., 2016). A second application for wetland CH₄ models has been to quantify the climate response to wetland CH₄ emissions (Gedney et al., 2004, 2019; Zhang et al., 2017b). In this case, results from wetland CH₄ models are used in climate-carbon cycle model emulators to assess their impact on radiative forcing (Gedney et al., 2019; Zhang et al.,



2017b). These modelling studies have contributed to advance research on the possible evolution of wetland CH₄ emissions in the 21st century (Koven et al., 2011; Shindell et al., 2004), the magnitude of their impact on the global climate (Gedney et al., 2019; Zhang et al., 2017b), and their implications for international climate policy (Comyn-Platt et al., 2018). However, their quasi-coupling methods do not reflect the complete feedback loop between climate conditions and wetland CH₄ emissions as expected in the natural world. So far, only 1-D and 2-D models of the northern high-latitude regions have been applied for simulating the feedback between climate conditions (temperature changes) and wetland CH₄ emissions in a fully coupled mode (Schneider von Deimling et al., 2012, 2015).

The implementation of process-based wetland CH₄ models in fully coupled ESMs is needed in order to advance research on wetland CH₄-climate feedbacks in the context of global climate projections (Dean et al., 2018). In particular, this addition to Earth system modelling should be beneficial to ongoing research on the permafrost carbon feedback (Nzotungicimpaye and Zickfeld, 2017; Schuur et al., 2015) and the remaining carbon budget for achieving the goals of the Paris Agreement (Rogelj et al., 2019).

This paper introduces a wetland CH₄ model developed for implementation in ESMs and currently embedded in an Earth system model of intermediate complexity (EMIC). Our study aims at developing a computationally efficient process-based model for simulating large-scale wetland CH₄ emissions constrained with sparse observations. Section 2 gives an overview of processes regulating CH₄ emissions in wetlands. Section 3 provides the model description and an outline of performed model simulations. Section 4 describes the model calibration and choice of parameter values. Section 5 presents the model performance evaluation. Section 6 describes the model sensitivity to poorly constrained parameters. Sections 7 and 8 are for discussions and conclusions, respectively.

2 Overview of processes regulating methane emissions in wetlands

2.1 Microbial production of methane

Wetlands host several communities of microbes adapted to the predominant anoxic conditions of these environments (Bridgham et al., 2013). Some of these microbes are methanogens, which decompose organic matter for their metabolism and produce CH₄ as a by-product of their respiration (McCalley et al., 2014; Segers, 1998). The organic matter decomposed by methanogens in wetlands originates from litter-fall, root exudates, dead plants and dissolved organic carbon (Bridgham et al., 2013; Conrad, 2009; Girkin et al., 2018; Mitsch and Mander, 2018). In the northern permafrost region, carbon from thawed soils constitutes an additional source of organic matter to methanogens (Kwon et al., 2019; Olefeldt et al., 2013).

There are three pathways through which methanogens produce CH₄ from soil organic matter (Le Mer and Roger, 2001; Segers, 1998; Whalen, 2005). The first pathway is operated by methanogens that rely on acetate for their metabolism, resulting in the production of both CH₄ and carbon dioxide (CO₂) (Bridgham et al., 2013; Whalen, 2005). The second pathway is operated by methanogens that produce CH₄ through CO₂ reduction in the presence of hydrogen (Bridgham et al.,



2013). The third pathway is operated by methanogens that use methylated substrates (e.g. methanol, methylamines, and
90 dimethylsulfide) for their metabolism (Zalman et al., 2018).

Rates of CH₄ production in wetlands are generally highest in upper anoxic layers due to several factors such as the
quality of organic matter and the spread of active microbial populations. For instance, in comparison to soil layers at depth
where organic matter can be recalcitrant to microbial decomposition, the organic matter in near-surface soil layers is more
labile due to fresh inputs from litter-fall and vegetation mortality (Treat et al., 2015; Walz et al., 2017; Wild et al., 2016).
95 Furthermore, observations at various sites show that methanogenic activity decreases as depth increases (Bridgham et al.,
2013; Cadillo-Quiroz et al., 2006).

Increasing soil temperatures stimulate the dynamics and growth of methanogenic communities in wetlands,
resulting in an increase of CH₄ production rates (Bridgham et al., 2013; Segers, 1998). However, several studies indicate that
there is an optimal temperature for methanogenic activity between 25°C and 30°C (Dean et al., 2018; Dunfield et al., 1993).
100 Other factors promoting the occurrence of CH₄ production in wetlands include the persistence of anoxic conditions as well as
soil pH varying between acidic and neutral (Dunfield et al., 1993; Segers, 1998).

2.2 Microbial oxidation of methane

In wetlands, methanotrophs (CH₄-oxidizing microbes) populate oxic portions of the soil column (Bridgham et al., 2013;
Conrad, 2009; Whalen, 2005). Such oxic portions are primarily soil layers close to the surface which are in contact with the
105 atmosphere, commonly near and above the water table (Bridgham et al., 2013; Le Mer and Roger, 2001; Segers, 1998). In
the presence of vascular plants, other oxic portions of the soil column can be found near the roots due to the downward
transport of oxygen (O₂) through plant aerenchyma (Kwon et al., 2019; Whalen, 2005). All these oxic portions of the soil
column constitute the so-called oxic zone, which is predominantly made of soil layers near and above the water table
(Bridgham et al., 2013; Conrad, 2009; Segers, 1998). Methanotrophs consume CH₄ that ascends from the zones of
110 production at depth to the overlying oxic zone for their metabolism, and primarily produce CO₂ as part of their respiration
(Bridgham et al., 2013; Segers, 1998).

While O₂ has been considered for years to be the only electron acceptor involved in the microbial oxidation of CH₄,
there is a growing evidence of the occurrence of CH₄ oxidation under anoxic conditions operated by anaerobic microbes that
rely on alternate electron acceptors such as nitrate and sulfate (Dean et al., 2018). However, although anaerobic CH₄
115 oxidation in marine environments has been well established for decades (Hoehler et al., 1994; Reeburgh, 1976), this process
remains poorly investigated in wetlands despite its potential importance for the CH₄ cycle (Gauthier et al., 2015; Smemo and
Yavitt, 2011).

In analogy to CH₄ production, CH₄ oxidation is influenced by changes in soil temperatures (Bridgham et al., 2013;
Segers, 1998). For instance, CH₄ oxidation rates increase during the summer because of intensified microbial activity but
120 also the availability of substantial CH₄ in response to increased soil temperatures (Segers, 1998). However, the temperature



response for CH₄ oxidation is generally lower than that for CH₄ production (Bridgham et al., 2013; Dean et al., 2018; Dunfield et al., 1993; Segers, 1998).

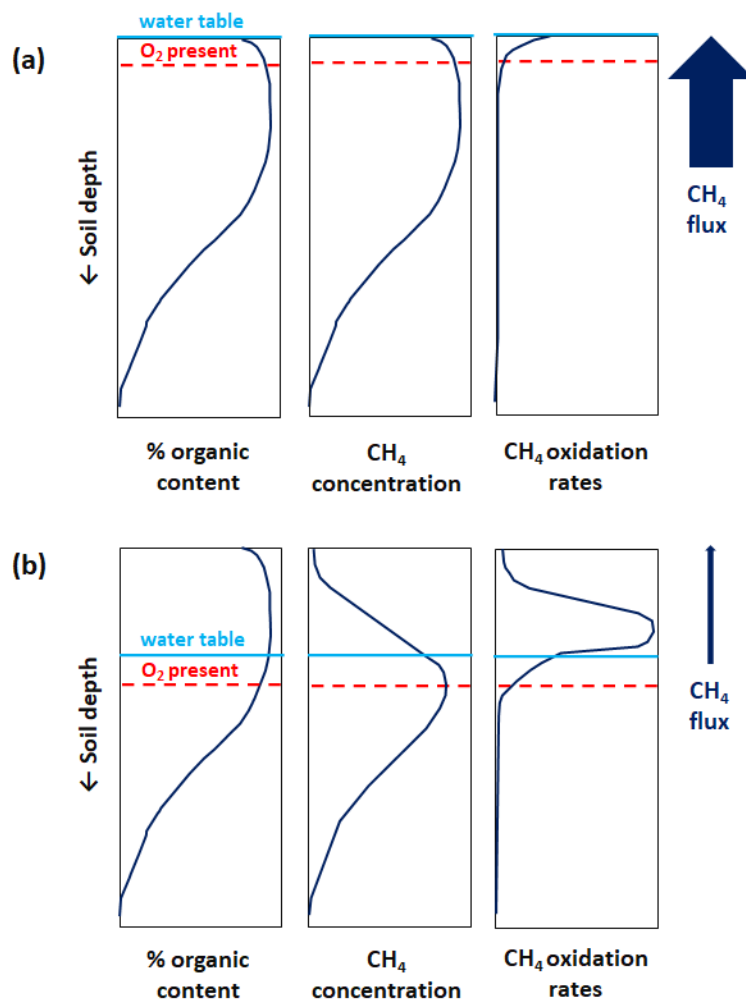
2.3 Mechanisms transporting methane to the atmosphere

There exist various mechanisms transporting CH₄ produced in wetlands to the atmosphere. Three transport mechanisms are well documented in the literature and generally monitored in situ (Bridgham et al., 2013; Whalen, 2005): the diffusion of CH₄ whereby molecules of CH₄ slowly ascend the overlying water column, the ebullition of CH₄ whereby bubbles of CH₄ rapidly ascend towards the soil surface, as well as the transport of CH₄ through the aerenchyma of vascular plants. However, other transport mechanisms for CH₄ in wetlands have been revealed: the hydrodynamic transport of CH₄ in the form of upwelling caused by temperature gradients primarily at nighttime (Poindexter et al., 2016), and the transport of CH₄ through tree stems (Bridgham et al., 2013; Conrad, 2009; Pangala et al., 2017) whose driving processes are still not well understood (Barba et al., 2019).

Methane oxidation is highly dependent on the predominant transport mechanism for CH₄. The water table position plays a crucial role in affecting what fraction of the produced CH₄ reaches the atmosphere (Blodau, 2002; Moore and Roulet, 1993; Segers, 1998). When the water table is well below the surface, methanotrophs may oxidize all of the diffusing CH₄ before the gas reaches the atmosphere (Segers, 1998). In the presence of vascular plants, a lower fraction of the produced CH₄ is oxidized because these plants allow the gas to bypass the oxic zone where methanotrophs are hosted (Blodau, 2002; Bridgham et al., 2013; Segers, 1998). In the case of ebullition, which often occurs episodically, CH₄ may escape to the atmosphere with reduced opportunities for oxidation (Bridgham et al., 2013; Whalen, 2005). How CH₄ oxidation relates to the transport of CH₄ through tree stems (Barba et al., 2019) or by hydrodynamic processes (Poindexter et al., 2016) is not well established.

2.4 A synopsis of wetland methane dynamics

Fig. 1 illustrates vertical profiles of soil organic content, CH₄ concentration, and CH₄ oxidation rates in a soil column with and without inundation at the surface based on principles outlined in the literature (Blodau et al., 2004; Whiticar and Faber, 1985). In general, the water table position determines the maximum depth at which O₂ is available in the soil column (i.e. the oxic-anoxic interface). When the surface is flooded and the water is stagnant (Fig. 1a), O₂ diffuses slowly into the soil column and may only be present in a portion of the upper soil layer which is in contact with the atmosphere. Under such predominantly anoxic conditions, CH₄ production occurs throughout the soil column and the concentration of CH₄ mirrors soil organic content – eventually with a small reduction near the surface due to CH₄ oxidation. A modest amount of ascending CH₄ may be oxidized throughout the soil column, but with highest oxidation rates near the surface where some O₂ may be available as an electron acceptor. The combination of high CH₄ production and only modest CH₄ oxidation in the soil column results in large CH₄ emissions into the atmosphere.



155 **Figure 1: Illustrated vertical profiles of soil organic content, CH₄ concentration and oxidation rates in a soil column with inundation at the surface (a) and without inundation at the surface (b). The vertical profiles are based on principles outlined in the literature (Blodau et al., 2004; Whiticar and Faber, 1985). For simplicity, the soil organic content is assumed to be identical in (a) and (b). In each case, the blue horizontal line illustrates the water table position and the dashed red horizontal line illustrates the oxic-anoxic interface or maximum depth at which O₂ is available in the soil column. The relative magnitude of CH₄ flux in the soil column is shown by the upward arrow to the right, also characterizing the relative magnitude of CH₄ emissions into the atmosphere.**

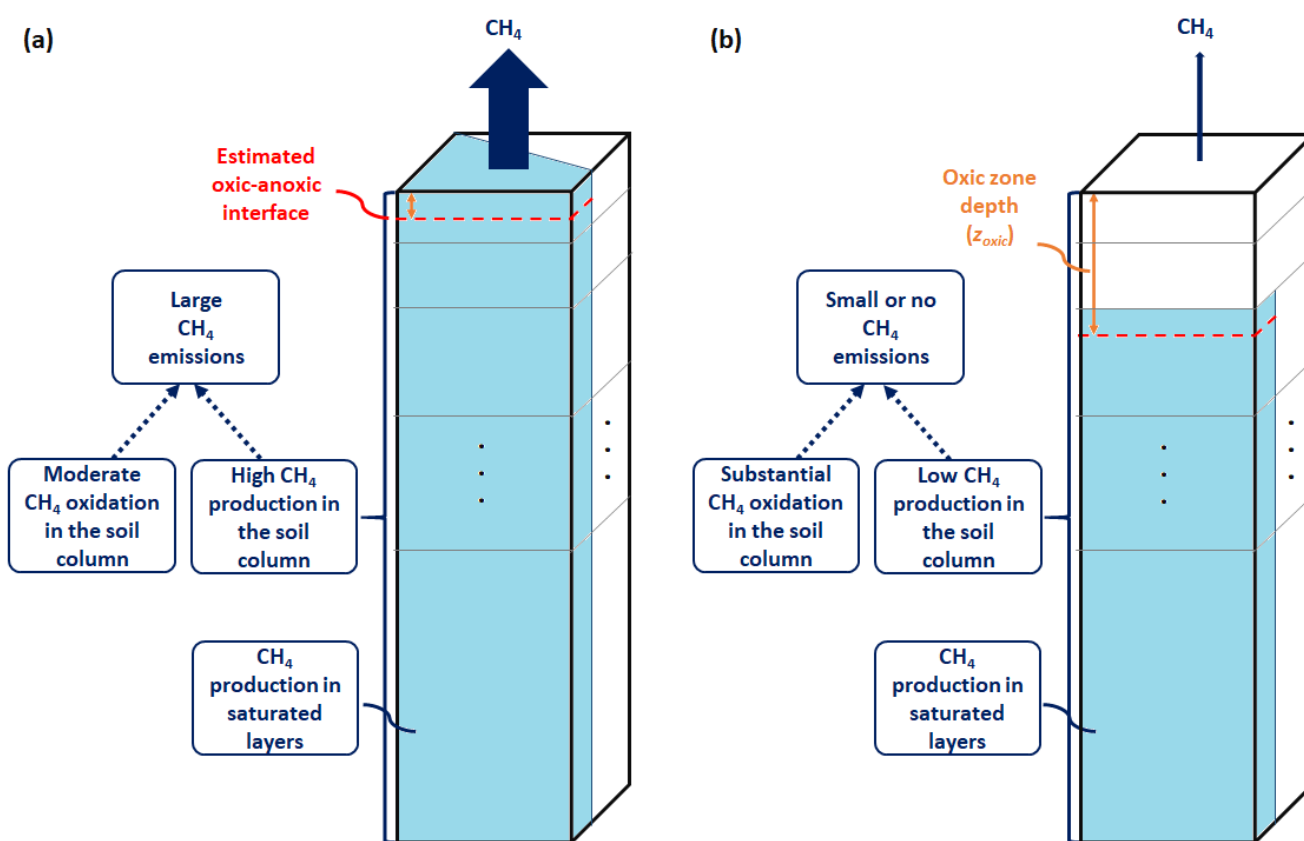
160 When the flooding recedes, O₂ becomes more prevalent in the upper soil column where CH₄ concentration decreases following a slow down or shut down of CH₄ production as aerobic microbes dominate the competition for organic matter (Fig. 1b). CH₄ production persists below the oxic-anoxic interface where the concentration of CH₄ mirrors soil organic content owing to the predominant anoxic conditions. Ascending CH₄ becomes subject to substantial oxidation in the soil column with the highest oxidation rates above the oxic-anoxic interface where O₂ is abundant. The combination of
165 decreased CH₄ production and substantial CH₄ oxidation in the soil column results in small or no CH₄ emissions into the atmosphere.



3 Model description and simulations

3.1 The wetland methane model: WETMETH

170 Microbial production and oxidation of CH_4 are parameterized in WETMETH using a multi-layer ground structure with information on the moisture distribution, the amount of organic matter (carbon content), and the average temperature in each soil layer. These soil variables are commonly simulated by ESMs. Fig. 2 provides a schematic representation of WETMETH for a soil column with and without inundation at the surface. By configuration, it is considered that CH_4 emissions in WETMETH may occur not only from inundated locations, but also from non-inundated ecosystems with a relatively high level of soil moisture content (Saunois et al., 2016, 2020).



175

180

Figure 2: Illustration of the developed wetland CH_4 model (WETMETH) and the dynamics of wetland CH_4 processes as represented in the model. This schematic representation depicts a soil column (model grid box) with inundation at the surface (a) and without inundation at the surface (b). The soil column is shown here with multiple layers of unequal thicknesses. The blue area at the surface of (a) represents the inundated surface area. The blue sections in the different soil layers of (a) and (b) represent water-saturated zones. For both (a) and (b), the dashed red horizontal line illustrates the oxic-anoxic interface and the orange vertical arrow shows the relative thickness of the oxic zone or oxic zone depth (z_{oxic}). Larger CH_4 emissions are expected to occur when the soil surface is flooded than when it is not due to relatively high CH_4 production and moderate CH_4 oxidation in the soil column.



3.1.1 Parameterization of methane production

185 For any land location, the rate of CH₄ production in an underlying soil layer i (P_i in kg C m⁻³ s⁻¹) is parameterized as:

$$P_i = S(\theta_i) C_j r Q_{10}^{\frac{T_i - T_0}{10}} \exp\left(-\frac{z_i}{\tau_{\text{prod}}}\right), \quad (1)$$

where $S(\theta_i)$ is the fraction of soil layer that is saturated with water, and C_j is the amount of soil carbon (in kg C m⁻³) in the layer. The product of $S(\theta_i)$ and C_j represents the organic matter (in kg C m⁻³) available for microbial decomposition under anoxic conditions. When the soil surface is not flooded (Fig. 2b), dry soil layers ($S(\theta_i) = 0$) are assumed to be predominantly
190 oxic and not producing CH₄ ($P_i = 0$) mostly due to aerobic microbes dominating the competition for organic matter which results in the starvation of methanogens (Segers, 1998).

The global factor r is the specific CH₄ production rate (in kg kg⁻¹ s⁻¹), which can be defined as the mass of CH₄-C that is produced per kilogram of available soil C per unit of time. A meta-analysis of incubated soil samples from various anaerobic landscapes indicates that r can vary between 0.3 to 27.2 μg of CH₄-C per g of soil C per day (equivalent to the
195 range from 3.5×10^{-12} to 3.1×10^{-10} kg kg⁻¹ s⁻¹) depending on the landscape type, relative water table position, and soil depth (Treat et al., 2015). Section 4.1 discusses the choice of the value for r as part of the model calibration.

The expression $Q_{10}^{\frac{T_i - T_0}{10}}$, which depends on the average layer temperature T_i (in Kelvin, K) and a baseline temperature T_0 (273.15 K), represents the temperature-dependency of CH₄ production expressed with a Q_{10} coefficient as commonly done to approximate the sensitivity of biological processes to a temperature change of 10 K (Hegarty, 1973).
200 While some biological processes double in rate with a warming of 10 K, several studies report a higher temperature sensitivity for CH₄ production (i.e. $Q_{10} > 2$) although with large uncertainties (Lupascu et al., 2012; Sjögersten et al., 2018; Walz et al., 2017; Whalen, 2005). Nevertheless, a meta-analysis of temperature-response studies suggests an average Q_{10} of about 4.2 for CH₄ production in pure cultures of methanogens (Hoehler and Alperin, 2014; Yvon-Durocher et al., 2014) in agreement with previous estimates (Blodau, 2002). In order to account for uncertainties with this coefficient and define the
205 occurrence of an optimal temperature for CH₄ production (Blake et al., 2015; Dean et al., 2018; Dunfield et al., 1993), a temperature-dependent Q_{10} is considered in WETMETH. Its mathematical formulation is $Q_{10}(T_i) = 1.7 + 2.5 \tanh [0.1 (T_{ref} - T_i)]$, where $T_{ref} = 308.15$ K is a reference temperature (Table 1). This formulation is defined following an expression used for soil respiration in another study (Wu et al., 2016). Additional information on this formulation and its implications for the temperature-dependency of CH₄ production are provided in Appendix A1. Furthermore, CH₄ production
210 in WETMETH is assumed to shut down in frozen soil layers although research suggests that slow microbial activity can occur at temperatures below 273.15 K (Panikov and Dedysh, 2000; Rivkina et al., 2004).

The expression $\exp\left(-\frac{z_i}{\tau_{\text{prod}}}\right)$, which depends on the depth of the soil layer i relative to the surface (z_i in m, positive downwards), describes the declining effect of various environmental controls on CH₄ production with depth that are generally unresolved by ESMs. These environmental factors include the quality of organic matter and the spread of
215 methanogens among other factors (Bridgman et al., 2013; Koven et al., 2015; Treat et al., 2015; Walz et al., 2017; Wild et



al., 2016). Here, τ_{prod} (in m) is a scaling parameter for CH₄ production. The choice of the value for τ_{prod} is discussed later as part of the model calibration (see Section 4.1).

Table 1: Model parameters for methane production and oxidation.

Parameter	Description	Units	Chosen value
r	Specific CH ₄ production rate	kg kg ⁻¹ s ⁻¹	^a 2.6 x 10 ⁻¹⁰
Q_{10}	Temperature coefficient for CH ₄ production	—	^b 4.2
T_{ref}	Reference temperature for CH ₄ production	K	^c 308.15
τ_{prod}	Scaling parameter for CH ₄ production	m	0.75
z_{oztz}	Thickness of the oxic-anoxic transition zone	m	0.05
τ_{oxid}	Scaling parameter for CH ₄ oxidation	m	0.0146

^a This value is equivalent to 22.8 µg CH₄-C produced per g of soil C per day; ^b A temperature-dependent Q_{10} , approximating 4.2 for a wide range of temperatures, is used instead (see Appendix A1); ^c The reference temperature is used to define an optimal temperature for CH₄ production (see Appendix A1).

The total amount of CH₄ produced in the soil column (P in kg C m⁻² s⁻¹) is calculated as:

$$P = \int_{i=1}^{i=k} P_i dz_i, \quad (2)$$

where P_i (in kg C m⁻³ s⁻¹) is the rate of CH₄ production in the soil layer i from Eq. (1), dz_i (in m) is the thickness of the soil layer i , and k represents the bottom-most soil layer. This amount of CH₄ (P) is then subject to oxidation in transit to emission into the atmosphere.

3.1.2 Parameterization of methane oxidation and net methane emissions

Methane oxidation is parameterized based on the amount of CH₄ produced in the soil column and the relative thickness of the oxic zone. Specifically, the total amount of CH₄ oxidized in the soil column (O_x in kg C m⁻² s⁻¹) and net CH₄ emissions to the atmosphere (E in kg C m⁻² s⁻¹) are calculated as:

$$O_x = P \left(1 - \exp\left(-\frac{z_{\text{oxic}}}{\tau_{\text{oxid}}}\right) \right), \quad (3)$$

$$E = P - O_x, \quad (4)$$

which is equivalent to the following expression:

$$E = P \exp\left(-\frac{z_{\text{oxic}}}{\tau_{\text{oxid}}}\right), \quad (5)$$

where P (in kg C m⁻² s⁻¹) is the total amount of CH₄ produced in the soil column as defined in Eq. (2), z_{oxic} (in m) is the relative depth (positive downwards) to the oxic-anoxic interface (Fig. 2), and τ_{oxid} (in m) is a scaling parameter for CH₄ oxidation. As for τ_{prod} , the choice of the value for τ_{oxid} is discussed as part of the model calibration (see Section 4.2).

Regarding z_{oxic} , we assume that O₂ may be present in soil layers unsaturated with water as well as in a shallow oxic-anoxic transition zone within the upper-most soil layer saturated with water (Fig. 2). In this first development of WETMETH, we consider a constant thickness (z_{ozatz}) of 0.05 m for the oxic-anoxic transition zone (Frolking et al., 2002;



Singleton et al., 2018). The penetration of O₂ into the soil and its dynamics with changing moisture conditions can be complex depending on site-specific factors such as the soil composition (Estop-Aragonés et al., 2012) and the presence of vascular plants (Brune et al., 2000). In addition, methanotrophs may be present at depth (> 0.05 m) below the water table probably following some adaptation to low O₂ conditions (Singleton et al., 2018). Nevertheless, the approach applied here for z_{oxic} is reasonable for ESMs not resolving O₂ dynamics and microbial communities in the soil.

For Eq. (3), the expression $(1 - \exp(-\frac{z_{\text{oxic}}}{\tau_{\text{oxid}}}))$ represents the fraction of P that gets oxidized in transit to emission into the atmosphere. Various studies report estimates of CH₄ oxidation as a fraction of produced CH₄ in the soil column (Blazewicz et al., 2012; Le Mer and Roger, 2001; Roslev and King, 1996; Segers, 1998; Singleton et al., 2018). From sample-to-sample and site-to-site, however, CH₄ oxidation exhibits a broad range of values ranging from less than 20% to more than 95% depending on the sampled soil depth ranges, whether or not potential CH₄ oxidation under anoxic conditions is considered, the monitored transport mechanisms for CH₄ among many other factors (Blazewicz et al., 2012; Couwenberg et al., 2010; Jauhiainen et al., 2005; Kwon et al., 2019; Le Mer and Roger, 2001; Moosavi and Crill, 1998; Roslev and King, 1996; Segers, 1998; Singleton et al., 2018; Whalen, 2005). Nevertheless, the largest fractions of oxidized CH₄ are generally associated with the deepest water tables or oxic-anoxic interfaces (Bridgham et al., 2013; Couwenberg et al., 2010; Jauhiainen et al., 2005; Roslev and King, 1996; Segers, 1998; Whalen, 2005).

The parameterization described in Eq. (3) is a simple approach for characterizing CH₄ oxidation in the soil column. Such a parameterization is practical when there is little knowledge on the soil chemistry (e.g. O₂ and alternate electron acceptors), the dynamics of methanotrophs and other environmental factors exerting a control on CH₄ oxidation (Blazewicz et al., 2012; Blodau, 2002; Dean et al., 2018; Kwon et al., 2019; Singleton et al., 2018; Smemo and Yavitt, 2011). Most importantly, this parameterization considers the net effect of all mechanisms transporting CH₄ from the anoxic soil layers where the gas is produced to the atmosphere. The oxidized CH₄ is assumed to produce CO₂ that becomes part of the soil respiration routinely simulated by ESMs.

3.2 The embedding Earth system model

WETMETH has been embedded in the University of Victoria Earth System Climate Model (UVic ESCM), an Earth system model of intermediate complexity (EMIC) (Weaver et al., 2001). A modified version of the EMIC based on UVic ESCM 2.9 (Eby et al., 2009) is used here. The UVic ESCM consists of a 3-D ocean general circulation model that is coupled to a dynamic-thermodynamic sea ice model, a 2-D (vertically-integrated) energy-moisture balance model for the atmosphere and a land surface model (Weaver et al., 2001). The land surface model is a modified version of the Met Office Surface Exchange Scheme (MOSES) with 14 ground layers of unequal thickness extending down to a depth of 250 m that can simulate permafrost processes such as freeze-thaw dynamics (Avis et al., 2011). The top eight ground layers (~10 m in total depth) are soil layers and contribute to the water cycle, whereas the bottom six ground layers are bedrock layers (Avis et al., 2011). In the hydraulically active layers, porosity and permeability are determined based on the relative abundance of



prescribed sand, clay, and silt-sized particles. Water phase changes are determined over a range of soil temperatures to
275 determine the fraction of frozen and unfrozen water in the ground (Avis et al., 2011). All components of the UVic ESCM
have a horizontal grid resolution of 3.6° in longitude and 1.8° in latitude (Eby et al., 2009; Weaver et al., 2001).

Wetlands in the UVic ESCM are identified in grid cell areas based on soil moisture content and topography. Model
grid cells in which wetlands can occur are those with unfrozen soil moisture contents greater than 65% of the saturated
moisture content in the upper soil layer for at least one day in a year (Avis et al., 2011). Instead of using a fixed global
280 threshold value for topography (Avis et al., 2011), the version of the UVic ESCM used here identifies wetland coverage at
the sub-grid scale following a TOPMODEL approach for global models (Gedney and Cox, 2003). Appendix A2 describes a
minor modification applied to this TOPMODEL approach. Section 5.1 presents an evaluation of wetlands simulated by the
UVic ESCM.

The UVic ESCM includes a representation of the global carbon cycle. The terrestrial carbon cycle is simulated
285 using the Top-down Representation of Interactive Foliage and Flora including Dynamics (TRIFFID), a dynamic global
vegetation model that is coupled to the land surface model (Avis et al., 2011; Meissner et al., 2003). TRIFFID defines the
state of the terrestrial biosphere in terms of soil carbon as well as the structure and coverage of five plant functional types
(PFTs): broadleaf trees, needleleaf trees, shrubs, C3 grasses and C4 grasses (Cox, 2001; Matthews et al., 2004; Meissner et
al., 2003). Terrestrial carbon gain occurs through photosynthesis that is simulated as a function of atmospheric CO₂
290 concentration, shortwave radiation, air temperature, humidity, and soil moisture. Soil carbon gain occurs through litter-fall
and vegetation mortality. The present-day permafrost carbon pool is simulated by the UVic ESCM following a method that
approximates the effect of long-term freeze-thaw cycles on the vertical distribution of carbon in permafrost-affected soils, a
process referred to as cryoturbation (MacDougall and Knutti, 2016). Soil carbon can occur in the top six ground layers
(~3.35 m in total depth). Terrestrial carbon loss occurs through autotrophic respiration by plants and heterotrophic
295 respiration by soil microbes (Matthews et al., 2004; Meissner et al., 2003). By configuration, permafrost carbon can only be
lost through microbial respiration and this heterotrophic respiration is assumed to shut down in frozen soil layers
(MacDougall et al., 2012; MacDougall and Knutti, 2016).

The marine carbon cycle in the UVic ESCM is represented with organic and inorganic carbon cycle models (Eby et
al., 2009). The organic carbon cycle is based on marine biology simulated with a nutrient-phytoplankton-zooplankton-
300 detritus (NPZD) ecosystem model (Schmittner et al., 2008). The inorganic carbon cycle model simulates the air-sea
exchange of CO₂ and ocean carbonate chemistry following the protocols of the Ocean Carbon-Cycle Model Intercomparison
Project (OCMIP) (Orr, 1999; Weaver et al., 2001). Dissolved inorganic carbon is treated as a passive tracer that is subject to
ocean circulation (Weaver et al., 2001). Carbonate dissolution in ocean sediments is simulated with a model of respiration in
marine sediments (Archer, 1996; Eby et al., 2009).



305 3.3 Model simulations

For this research, three series of model simulations are performed with the UVic ESCM in its standard fully coupled mode and including WETMETH parameterizations:

1. Firstly, the UVic ESCM is spun up for ~5000 years at year 1850 conditions to allow the model to reach an equilibrium climate state representing the pre-industrial period.
- 310 2. Secondly, a transient run from 1850 to 2019 is performed in order to evaluate the model performance. This transient run is based on prescribed CO₂ concentration and other forcing data from the fifth phase of the Coupled Model Intercomparison Project (CMIP5) (Taylor et al., 2012). The UVic ESCM is driven by historical data from 1850 to 2005 and by Representative Concentration Pathway (RCP) 8.5 data from 2006 to 2019. Supplementary Fig. S1 illustrates how the simulated historical climate conditions compare to observations in terms of global mean surface
315 air temperature.
3. Thirdly, a set of transient runs from 2000 to 2009 is performed to analyze the model sensitivity to poorly constrained parameters. This set of model simulations (sensitivity runs) is performed by perturbing values of poorly constrained parameters associated with wetland CH₄ processes.

4 Choice of model parameter values

320 Here, we describe the choice of three WETMETH parameters (r and τ_{prod} for CH₄ production; τ_{oxid} for CH₄ oxidation) as part of the model calibration. These model parameters are tuned to observations from northern high-latitude regions due to the scarcity of large-scale datasets from other regions. The model calibration against northern observations is based on the assumption that tuned parameter values will be valid across the globe, which is an important limitation as it will be discussed later. Nonetheless, this approach is deemed reasonable given the present state of data availability. Section 5.1 describes
325 northern wetlands simulated by the UVic ESCM as part of the model validation.

4.1 Methane production parameters

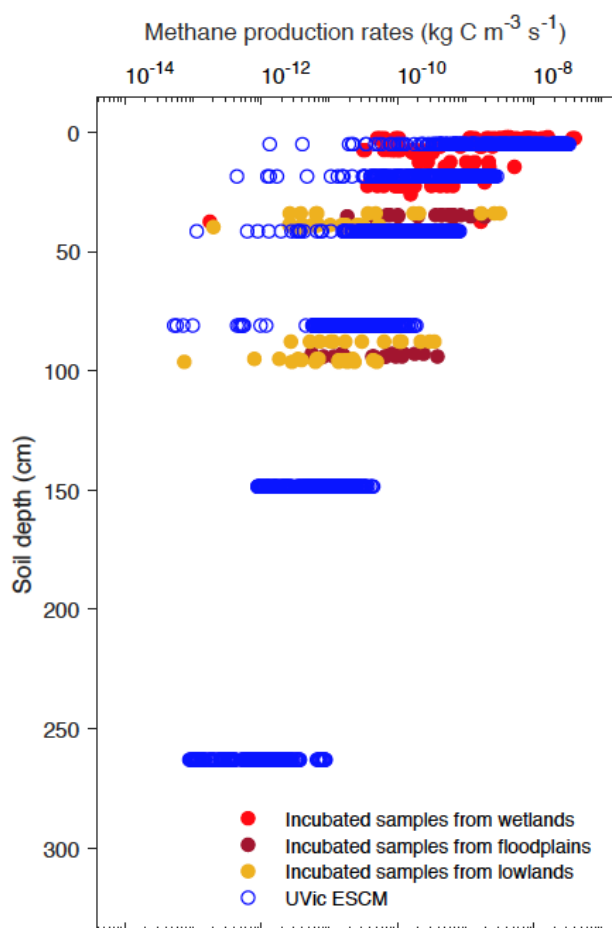
Parameters for CH₄ production in WETMETH are calibrated against maximum CH₄ production rates measured in laboratory incubations of soil samples from several anaerobic environments across northern high-latitude regions (>50°N). These potential CH₄ production rates are obtained from a synthesis dataset, which includes information on other environmental
330 variables such as the relative depth of the soil samples (Treat et al., 2015).

To allow a fair model-data comparison, measured CH₄ production rates with corresponding soil bulk density from the sites of origin are converted into units of kg C m⁻³ s⁻¹ (see Appendix A3). Furthermore, measurements from landscapes identified as uplands and lakes (in the dataset) are excluded from the dataset used in this model calibration. The remaining



335 measurements are potential CH₄ production rates in soil samples from landscapes identified (in the dataset) as wetlands,
floodplains and lowlands across Alaska.

In order to set values for r and τ_{prod} from Eq. (1), the depth profile of simulated CH₄ production rates across Alaska
for the year 2000 is tuned to that of the measurements. By setting r to 22.8 $\mu\text{g CH}_4\text{-C}$ produced per g of soil C per C day
(equivalent to $2.6 \times 10^{-10} \text{ kg kg}^{-1} \text{ s}^{-1}$) and τ_{prod} to 0.75 m, we obtain a depth profile of simulated CH₄ production rates that
compares fairly well to that of potential CH₄ production rates from the laboratory incubations (Fig. 3). These default values
340 for r and τ_{prod} are listed in Table 1. Section 6 presents a sensitivity analysis on these model parameters.



345 **Figure 3: Vertical profiles of simulated and potential CH₄ production rates from wetlands across Alaska. Potential CH₄ production rates are measurements from laboratory incubations of soil samples collected from various anaerobic ecosystems (Treat et al., 2015). Both simulated and measured CH₄ production rates are shown here with a log-transformed axis (base-10 logarithmic scale).**



4.2. Methane oxidation parameter

Unlike for CH₄ production, there are no published large-scale measurements of CH₄ oxidation rates that could be used in this research for the calibration of CH₄ oxidation. For that reason, CH₄ oxidation in WETMETH is indirectly calibrated via CH₄ emissions. A synthesis dataset of seasonal and annual CH₄ emissions from various terrestrial sites across temperate, boreal and Arctic regions is used to this end (Treat et al., 2018). The model calibration focuses on annual CH₄ emissions from sites north of 50°N for which many data points are available in the dataset.

While most data points are from direct measurements of CH₄ emissions, some data points are associated with different modelling methods for estimating CH₄ emissions (Treat et al., 2018). To allow a fair model-data comparison, only data points associated with direct measurements of CH₄ emissions are included in the model calibration. Furthermore, measurements from lakes, uplands and alpine landscapes are excluded from this model calibration. In particular, the exclusion of data points from uplands and alpine landscapes sorts out measurements of terrestrial CH₄ uptake (negative CH₄ flux). The retained data points (n = 119) include measurements by chambers (85.7%), flux towers (13.4%) and a combination of flux towers and chambers (0.8%).

The model calibration in this section aims at choosing a value of τ_{oxid} from Eq. (5) such that the range (minimum - maximum) of annual CH₄ emissions across northern wetlands (>50°N) simulated by the UVic ESCM is comparable to that of annual CH₄ emissions from the data points (0.1-60.6 g CH₄ m⁻² yr⁻¹). By setting τ_{oxid} to 0.0146 m, we constrain simulated CH₄ emissions from northern wetlands (specifically, grid-cell CH₄ emissions divided by the inundated fraction of the grid cell) from 2000 to 2009 in the range of 0.04-65.6 g CH₄ m⁻² yr⁻¹. This default value for τ_{oxid} is listed in Table 1. Section 6 presents a sensitivity analysis on this model parameter.

5 Evaluation of the model performance

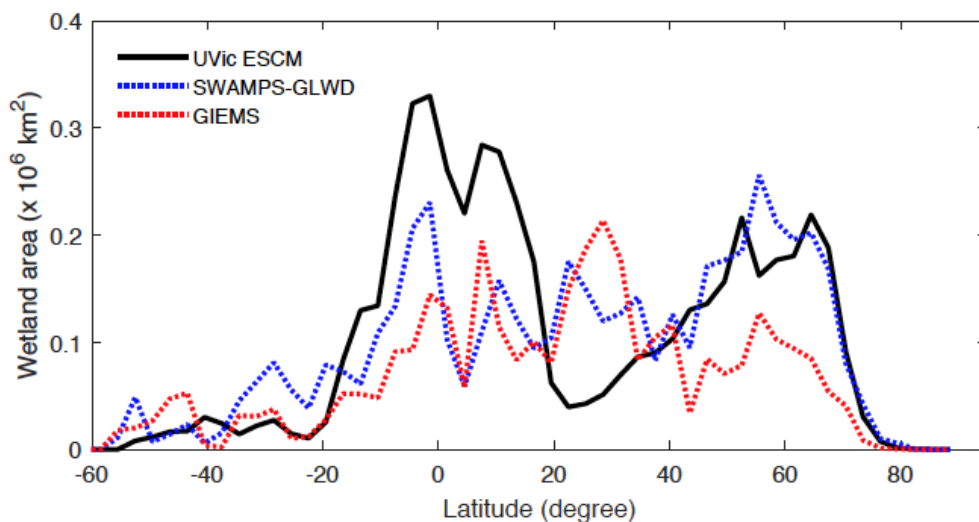
5.1 Wetlands

Fig. 4 shows the latitudinal distribution of wetland areas simulated by the UVic ESCM in comparison to two global datasets. The first dataset is Global Inundation Extent from Multi-Satellites (GIEMS), which is based on remotely sensed inundation areas (Papa et al., 2010; Prigent et al., 2001, 2007, 2012). The second dataset is Surface Water Microwave Product Series-Global Lakes and Wetlands Database (SWAMPS-GLWD), which is based on a combination of information from satellites and maps of inundated areas in order to reduce uncertainties associated with the distribution of global wetlands (Poulter et al., 2017). The comparison between the model and the datasets is done over 2000-2007, which is the overlap period for the datasets. Over this period the UVic ESCM simulates an annual maximal extent of ~12.6 million km² for global wetlands, whereas GIEMS and SWAMPS-GLWD estimate ~9.3 and ~10.6 million km², respectively.

The UVic ESCM agrees better with SWAMPS-GLWD in regions north of 40°N although with some underestimations around 55°N, and relatively well with GIEMS between 20-40°S (Fig. 4). However, the model simulates too



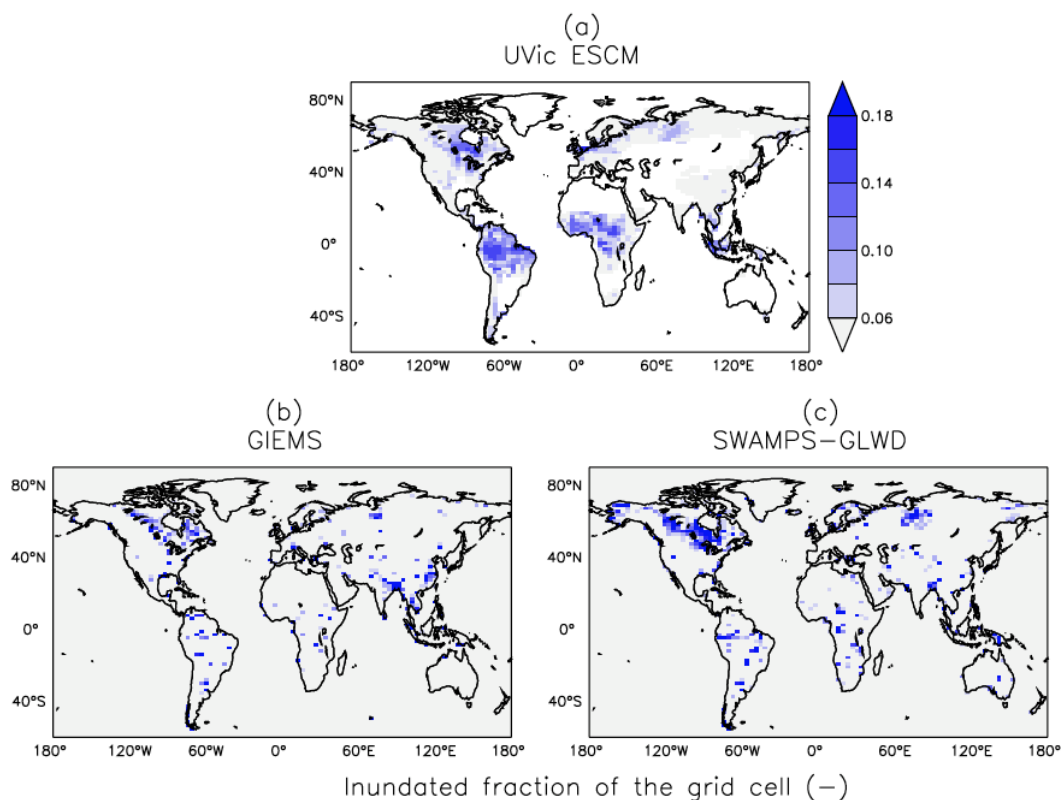
380 small wetland areas between 20-30°N when compared to both GIEMS and SWAMPS-GLWD. While our model could be underestimating wetland areas in this latitude zone, inundated areas estimated by GIEMS include rice paddies which prevail in tropical and sub-tropical regions (Prigent et al., 2007, 2012). Rice paddies are likely not represented in SWAMPS-GLWD as there were efforts to only include natural wetlands during the development of this dataset (Poulter et al., 2017). In comparison to GIEMS and SWAMPS-GLWD, our model simulates small wetland areas in South-East Asia especially near Bangladesh (Fig. 5 and Fig. 6).



385 **Figure 4: Latitudinal distribution of wetland areas simulated by the UVic ESCM over the 2000-2007 period in comparison to two global datasets: GIEMS and SWAMPS-GLWD. The comparison period corresponds to the overlap period for the two datasets. The wetland areas are summed across latitude bins of 3°.**

390 Between 20°N and 20°S, the UVic ESCM simulates a bimodal distribution of the wetland extent that is consistent with the two datasets although the model simulates too large wetland areas (Fig. 4). Unlike for GIEMS and SWAMPS-GLWD, wetlands simulated by the UVic ESCM are widespread in Amazonia, West and Central Africa (Fig. 5 and Fig. 6). Although the UVic ESCM could be overestimating the extent of wetlands in some of these equatorial regions, it is possible that GIEMS and SWAMPS-GLWD do not detect inundated areas in densely forested regions due to forest canopies. Recent studies suggest that tropical wetlands are commonly underestimated in large-scale datasets (Dargie et al., 2017; Gumbrecht et al., 2016).

395 Conversely, it is possible that the UVic ESCM overestimates tropical wetland areas due to soil hydraulic properties unrepresented in the model. A potential cause for the overestimation of tropical wetlands in our model is the standard approach for simulating global hydrology in land surface models based on the concentration of only sand, clay and silt in the soil. A recent study suggests that the inclusion of ferralsols (weathered soils with micro-aggregated particles that are common in the humid tropics) in a global terrestrial model can help improve the simulation of tropical wetlands (Gedney et al., 2019).

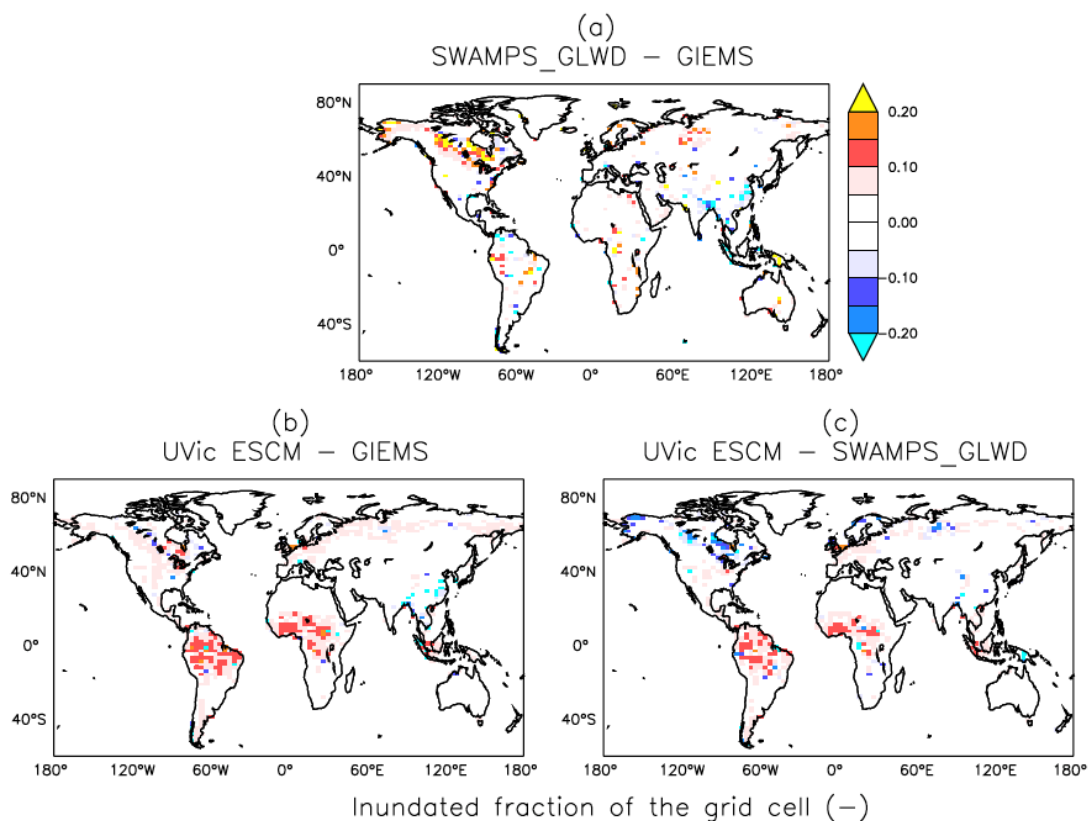


400

Figure 5: Average wetland extents (inundated fractions of grid cells) across the globe over the 2000-2007 period as simulated by the UVic ESCM (a) in comparison to two datasets: (b) GIEMS and (c) SWAMPS-GLWD. The datasets are regridded to $3.6^{\circ} \times 1.8^{\circ}$ for a fair comparison with the UVic ESCM. The comparison period corresponds to the overlap period for the two datasets.

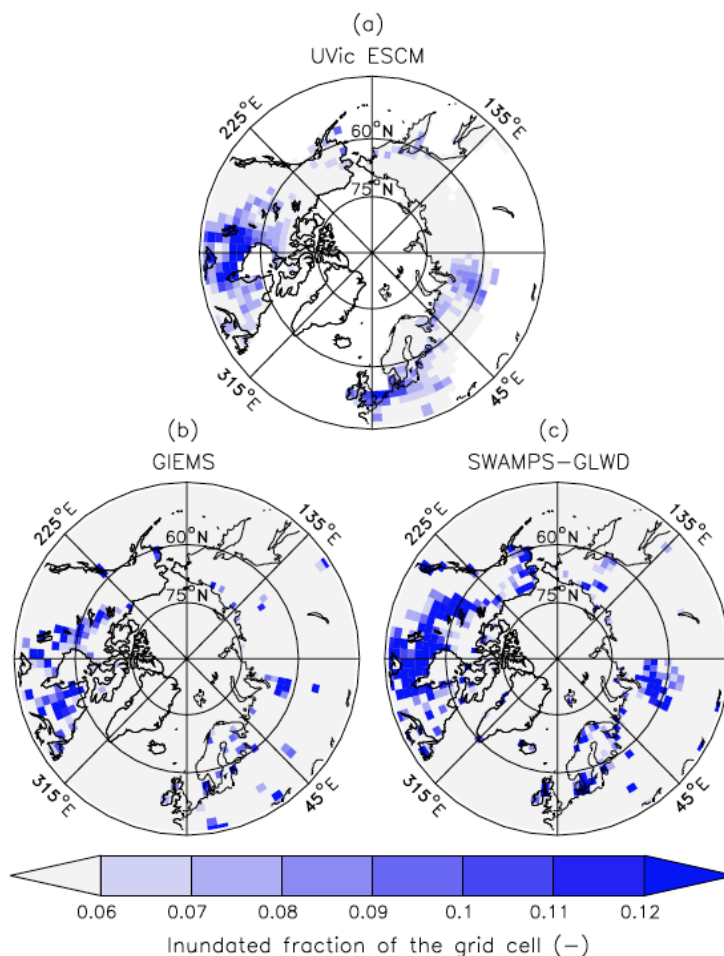
Outside of the tropics, the UVic ESCM does a better job at simulating the distribution of wetlands in sub-Arctic and Arctic regions (Fig. 7). The model simulates the occurrence of wetlands (i.e. surface inundation) across the West Siberian Lowlands (WSL) in Russia, the Hudson Bay Lowlands (HBL) in Canada as well as over other parts of northern Canada in agreement with both SWAMPS-GLWD and GIEMS (Fig. 7). However, some disagreements between the UVic ESCM and the two datasets can also be identified: (i) in comparison to GIEMS, the UVic ESCM simulates more wetland area in the Hudson Bay Lowlands (HBL) as well as widespread wetlands in parts of northern Eurasia (Fig. 7b and Fig. S2b); (ii) in comparison to SWAMPS-GLWD, the model simulates less wetland area over the WSL and northern Canada including the HBL and more wetland area in parts of Europe (Fig. 7c and Fig. S2c).

Statistical analyses show that: (i) the UVic ESCM agrees better with SWAMPS-GLWD than with GIEMS at both the regional and global scale; and (ii) the model compares better with the two datasets across northern regions than at the global scale. For details on the statistical evaluation, please see supplementary Table S1.



415

Figure 6: Differences in global wetland extents (inundated fractions of grid cells) between two datasets (GIEMS and SWAMPS-GLWD) and the UVic ESCM over the 2000-2007 period: (a) SWAMPS-GLWD – GIEMS, (b) UVic ESCM – GIEMS, and (c) UVic ESCM – SWAMPS-GLWD. The comparison period corresponds to the overlap period for the two datasets.



420 **Figure 7: Average wetland extents (inundated fractions of grid cells) in the north of 45°N over the 2000-2007 period as simulated**
425 **by the UVic ESCM (a) in comparison to two datasets: (b) GIEMS and (c) SWAMPS-GLWD. The datasets are regridded to 3.6° x**
1.8° for a fair comparison with the UVic ESCM. The comparison period corresponds to the overlap period for the two datasets.

5.2 Wetland methane emissions

Given the relative coarse grid resolution of the UVic ESCM, the model validation with respect to wetland CH₄ emissions
425 focuses on large-scale emissions such as regional, zonal, and global emissions. Moreover, this model validation focuses on
northern high-latitude regions because observations and estimates of wetland CH₄ emissions from other regions (e.g. the
tropics) are scarce. This focus is further justified by the fact that our model better simulates the distribution of wetlands in
northern high-latitude regions than in the tropics (see Section 5.1). Indeed, the extent of wetlands is a major control for
wetland CH₄ emissions simulated by process-based models and probably the primary contributor to related uncertainties
430 (Melton et al., 2013; Saunois et al., 2020; Zhang et al., 2017a).



5.2.1 Northern high-latitude emissions

The UVic ESCM simulates total CH₄ emissions from northern wetlands that are in the range of recent estimates. Over the 2013-2014 period, the model simulates mean annual emissions of 33.2 Tg CH₄ yr⁻¹ for wetlands north of 45°N (Table 2). These CH₄ emissions are consistent with estimates from recent upscaled flux measurements (UFMs) over the same period
 435 based on a random forest (RF) algorithm and three wetland maps (Peltola et al., 2019): 30.6 ± 9.2 Tg CH₄ yr⁻¹ (RF-DYPTOP), 31.7 ± 9.4 Tg CH₄ yr⁻¹ (RF-PEATMAP), and 37.6 ± 11.8 Tg CH₄ yr⁻¹ (RF-GLWD) (Table 2). Supplementary Table S2 shows that the UVic ESCM has no preferential agreement with one of the three UFMs.

Table 2: Mean annual wetland CH₄ emissions simulated by the UVic ESCM in comparison to estimated emissions from the literature. All emissions are reported in Tg CH₄ yr⁻¹ and uncertainties are provided for estimates from the literature. Three periods are used to allow a fair comparison between the UVic ESCM and estimates from the literature where possible: 2008-2017 as in the latest global CH₄ budget report (Saunois et al., 2020), 2013-2014 as for recent upscaled flux measurements across the northern high-latitudes (Peltola et al., 2019), and 1993-2004 as for the WETCHIMP model ensemble (Melton et al., 2013). Principal methods used in the different references for estimates are reported in the last column: Top-down (TD) methods including inverse models (IM), and bottom-up (BU) methods including upscaled measurements (UM) as well as process-based models (PM).
 440
 445

	Geographical delimitation	UVic ESCM period	UVic ESCM emissions	Estimated emissions	Reference for estimates	Method in reference
Hudson Bay	50 – 60°N;	2013-2014	2.9	2.3 ± 0.3	Pickett-Heaps et al., 2011	BU
Lowlands	75 – 96°W			2.4 ± 0.3	Miller et al., 2014	IM
				2.7 - 3.4	Thompson et al., 2017	IM
West Siberian	50 – 75°N;	2013-2014	4.1	3.9 ± 1.3	Glagolev et al., 2011	UM
Lowlands	60 – 95 °E			6.1 ± 1.2	Bohn et al., 2015 ^a	IM
				6.9 ± 3.6	Thompson et al., 2017	IM
Pan-Arctic	60°N – 90°N	2008-2017	17.3	7 – 16	Saunois et al., 2020	TD
Wetlands				2 – 18	Saunois et al., 2020	BU
Northern	40°N – 90°N	2008-2017	38.5	37.4 ± 7.2	Treat et al., 2018	BU
Wetlands	45°N – 90°N	2013-2014	33.2	30.6 ± 9.2	Peltola et al., 2019	UM
				31.7 ± 9.4	Peltola et al., 2019	UM
				37.6 ± 11.8	Peltola et al., 2019	UM
Tropical	30°S – 30°N	1993-2004	105.5	126 ± 31	Melton et al., 2013 ^a	PM
Wetlands				90 ± 77	Sjögersten et al. 2014	UM
Global	90°S – 90°N	2008-2017	158.6	155 – 200	Saunois et al., 2020	TD
Wetlands				102 – 182	Saunois et al., 2020	BU

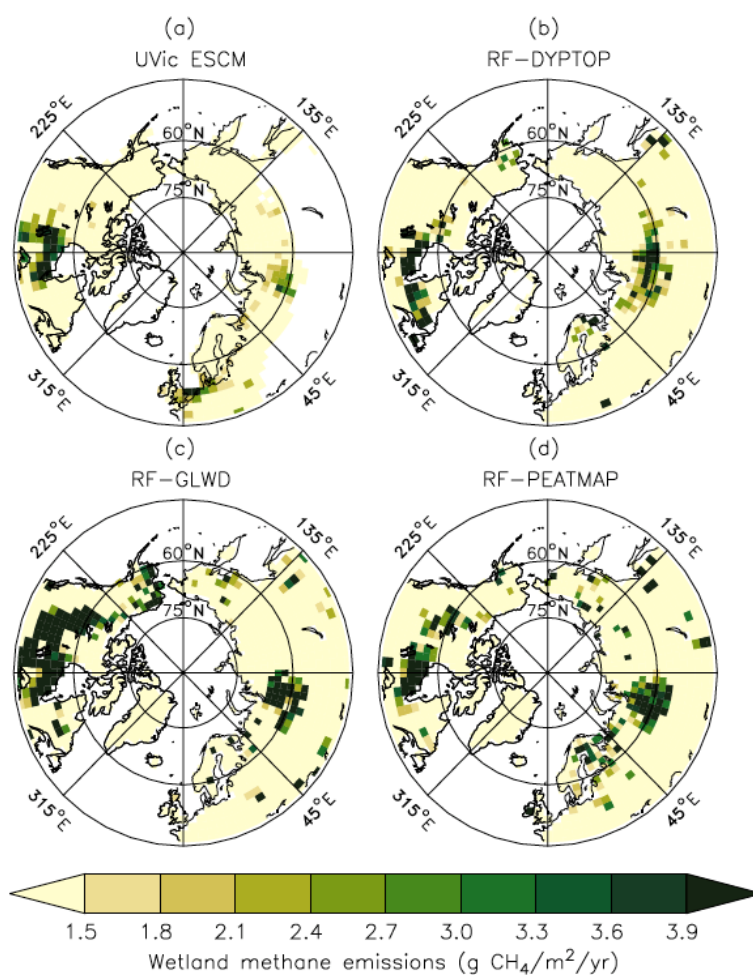
^a These reported estimates are model ensemble means. For the West Siberian Lowlands, the range between the inverse models is 3.1–9.8 Tg CH₄ yr⁻¹ (Bohn et al., 2015). For tropical wetlands, the range between the process-based models is 85–184 Tg CH₄ yr⁻¹ (Melton et al., 2013).

450 Fig. 8 shows the spatial distribution of simulated CH₄ emissions in comparison to the three UFMs. When compared to each other, the three UFMs exhibit substantial differences primarily attributed to the distinct wetland distributions (Peltola et al., 2019). Considering the general pattern and magnitude of wetland CH₄ emissions, the UVic ESCM agrees with either



two or all three UFM over key source regions such as the Hudson Bay Lowlands (HBL), the West Siberian Lowlands (WSL), western Europe and south-central Canada (Fig. 8).

455 The UVic ESCM simulates less CH₄ emissions over parts of northeastern Canada and Fennoscandia in comparison to the UFM (Fig. 8). However, the three UFM do not necessarily agree on both the distribution and magnitude of wetland CH₄ emissions in these regions. Furthermore, the UVic ESCM does not simulate wetland CH₄ emissions in southern Eurasia (40-135°E; 45-60°N) while the three UFM suggest that CH₄ can be emitted from sporadic wetlands in this region (Fig. 8). Overall, the mismatch between the UFM and our model in terms of northern CH₄ emissions can be primarily attributed to
460 differences in the wetland extent, but also to the spatial distribution of soil carbon simulated by the UVic ESCM (MacDougall and Knutti, 2016).



465 **Figure 8: Average CH₄ emissions from wetlands north of 45°N over the 2013-2014 period as simulated by the UVic ESCM (a) in comparison to three datasets (upscaled flux measurements): (b) RF-DYPTOP, (c) RF-GLWD and (d) RF-PEATMAP. The datasets are regridded to 3.6° x 1.8° for a fair comparison with the UVic ESCM. The comparison period corresponds to the overlap period for the three datasets.**



In terms of mean annual emissions from key source regions, the UVic ESCM simulates 2.9 Tg CH₄ yr⁻¹ for the Hudson Bay Lowlands (HBL) over the 2013-2014 period (Table 2). Although these emissions are lower than estimates by the three UFM (3.1-6.5 Tg CH₄ yr⁻¹) (Peltola et al., 2019), estimates by inverse models (2.0-3.4 Tg CH₄ yr⁻¹) over this region are comparable to our model results (Miller et al., 2014; Pickett-Heaps et al., 2011; Thompson et al., 2017). Furthermore, the UVic ESCM simulates total wetland emissions of 4.1 Tg CH₄ yr⁻¹ for the West Siberian Lowlands (WSL) over the 2013-2014 period (Table 2). Regional estimates based on the three UFM are higher (4.9-8.5 Tg CH₄ yr⁻¹) than our model results over the same period (Peltola et al., 2019), whereas previous observation-based estimates for the WSL suggest regional wetland emissions (3.9 ± 1.3 Tg CH₄ yr⁻¹) that are similar to our model results (Glagolev et al., 2011). Estimates by inverse models over the WSL are relatively high but comparable to our model estimates (Table 2): 6.1 ± 1.2 Tg CH₄ yr⁻¹ (Bohn et al., 2015) and 6.9 ± 3.6 Tg CH₄ yr⁻¹ (Thompson et al., 2017).

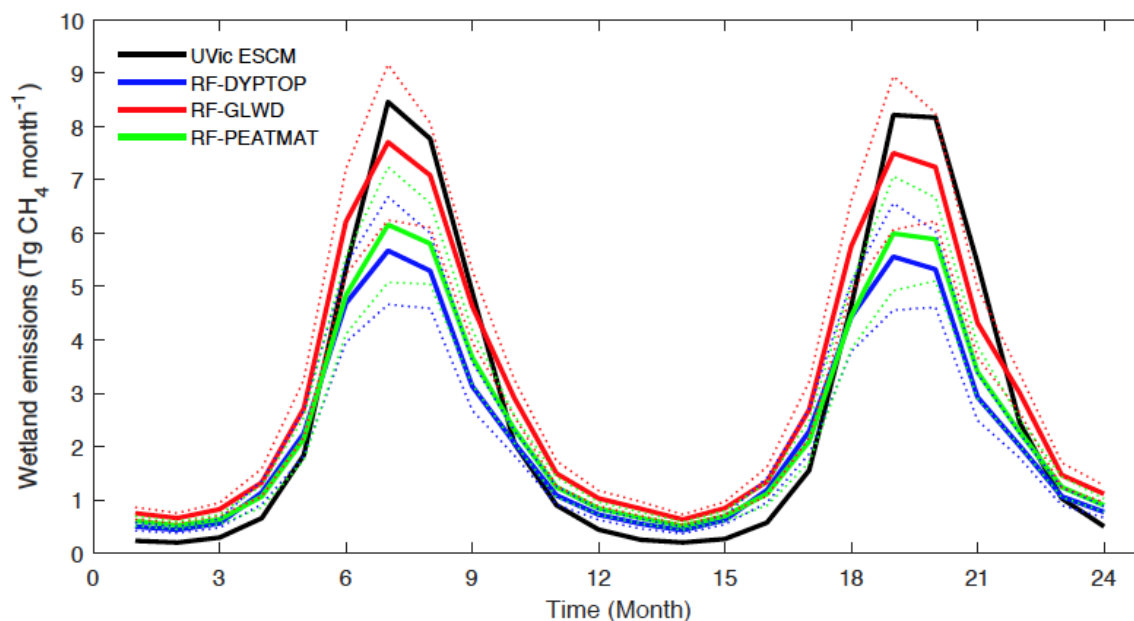
The UVic ESCM is also evaluated with respect to wetland CH₄ emissions over the 2000-2009 and 2008-2017 decades, which both are reference periods for the latest global CH₄ budget report (Saunois et al., 2020). For wetlands north of 40°N, the UVic ESCM simulates emissions of 37.7 Tg CH₄ yr⁻¹ over the 2000-2009 decade and 38.5 Tg CH₄ yr⁻¹ over the 2008-2017 decade. These wetland CH₄ emissions are consistent with recent estimates (37.4 ± 7.2 Tg CH₄ yr⁻¹) from data-constrained model ensembles over the same region (Treat et al., 2018). For wetlands north of 45°N, the model simulates total emissions that are in the range of estimates for the 2013-2014 period discussed earlier (32.4 Tg CH₄ yr⁻¹ over 2000-2009 and 33.1 Tg CH₄ yr⁻¹ over 2008-2017). For Pan-Arctic wetlands (>60°N), the UVic ESCM simulates emissions of 17.4 Tg CH₄ yr⁻¹ over the 2000-2009 decade and a similar amount over the 2008-2017 decade (Table 2). These wetland CH₄ emissions correspond to the upper limit of bottom-up estimates (2-18 Tg CH₄ yr⁻¹) from the latest global CH₄ budget report (Saunois et al., 2020).

Fig. 9 shows seasonal cycles of CH₄ emissions from wetlands north of 45°N over the 2013-2014 period as simulated by the UVic ESCM and estimated from the three UFM (Peltola et al., 2019). The pattern and magnitude of simulated seasonal emissions compare well to that of the UFM. For both the model and UFM, minimal emissions vary between 0.2-0.6 Tg CH₄ month⁻¹ and occur in December while peak emissions are well below 10 Tg CH₄ month⁻¹ and occur in July (Fig. 9). However, simulated peak emissions (~8.5 Tg CH₄ month⁻¹) are relatively higher than peak emissions for the UFM (range of best estimates: 5.6-7.5 Tg CH₄ month⁻¹). Moreover, in comparison to the three UFM, the UVic ESCM simulates lower CH₄ emissions between December and May but higher CH₄ emissions between July and September (Fig. 9).

The UVic ESCM simulates the occurrence of wetland CH₄ emissions during the non-growing season. For wetlands north of 45°N, our model simulates total emissions of 2.1 Tg CH₄ yr⁻¹ between November and March. The UFM predict total emissions of 4.6-10.2 Tg CH₄ yr⁻¹ during these cold months (Peltola et al., 2019). For wetlands north of 60°N, the UVic ESCM simulates emissions of 1.2 Tg CH₄ yr⁻¹ from October through May in agreement with recent estimates (1.6 ± 0.1 Tg CH₄ yr⁻¹) from data-constrained model ensembles for these months (Treat et al., 2018). Based on our calculations, the three UFM predict about 3.5-4.5 Tg CH₄ yr⁻¹ emitted from wetlands north of 60°N between October and May. Overall, this



500 analysis shows that WETMETH is capable of simulating non-negligible CH₄ emissions from northern wetlands during cold months as emphasized by recent studies (Treat et al., 2018; Zona et al., 2016).



505 **Figure 9:** Seasonal variations of CH₄ emissions from wetlands north of 45°N over the 2013-2014 period as simulated by the UVic ESCM in comparison to three upscaled flux measurements (RF-DYPTOP, RF-GLWD and RF-PEATMAP). The dashed lines show the uncertainty range for the upscaled flux measurements.

5.2.2 Global emissions

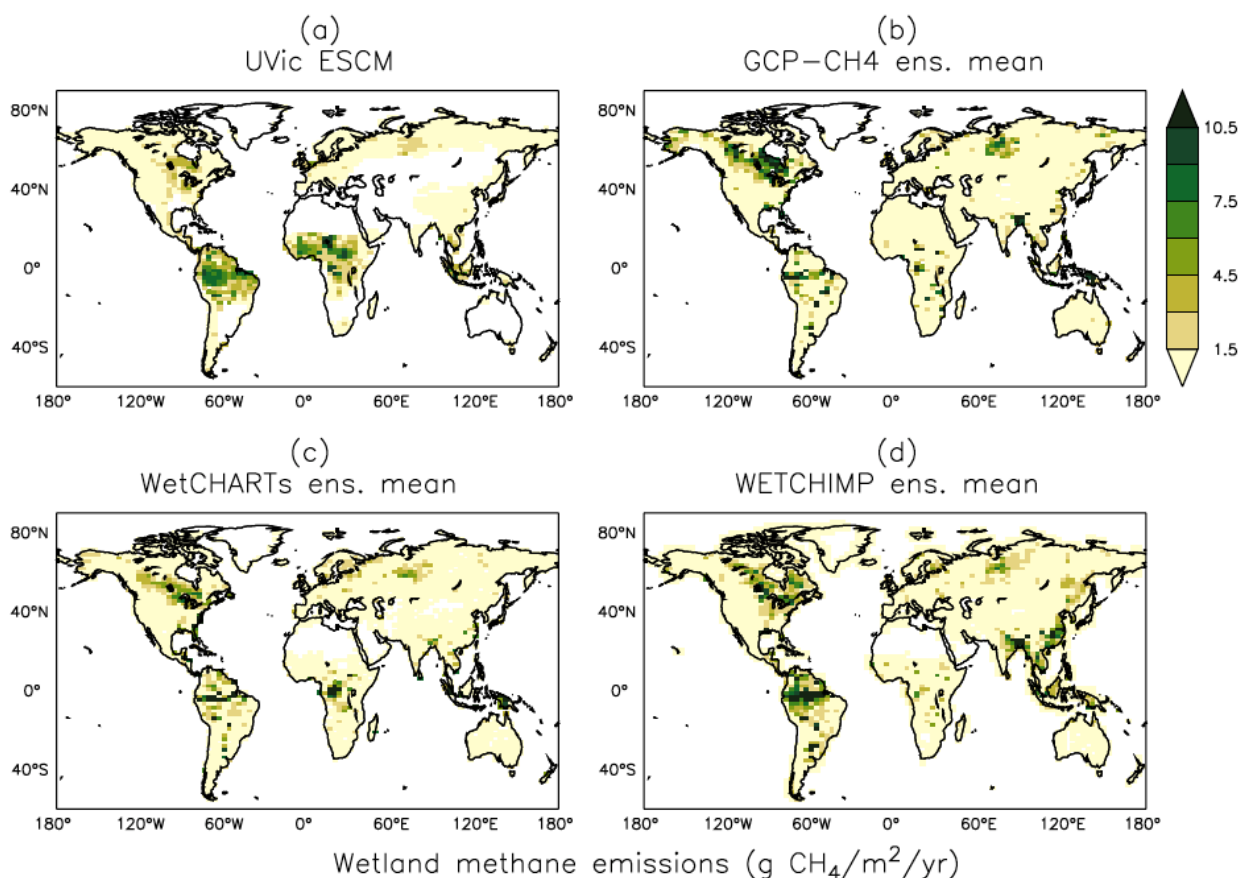
The UVic ESCM simulates total emissions of 155.1 and 158.6 Tg CH₄ yr⁻¹ from global wetlands over the 2000-2009 and 2008-2017 decades, respectively. According to the latest global CH₄ budget report, these wetland emissions are in the mid-range of bottom-up estimates (102-179 and 102-182 Tg CH₄ yr⁻¹) but close to the lower limit of top-down estimates (153-196 and 155-200 Tg CH₄ yr⁻¹) over the two decades (Saunois et al., 2020). Previous bottom-up estimates are significantly high (Melton et al., 2013; Saunois et al., 2016) primarily due to possible double counting of emissions from wetlands and other inland water areas (Saunois et al., 2020; Thornton et al., 2016) in addition to uncertainties associated with the extent of wetlands and model parameterizations (Melton et al., 2013). Table 2 summarizes the comparison between the model results and estimates from the latest global CH₄ budget report for the 2008-2017 decade.

515 Fig. 10 shows the spatial distribution of simulated wetland CH₄ emissions over the 2001-2004 period in comparison to three process-based model ensembles: GCP-CH₄ (Poulter et al., 2017), WetCHARTs (Bloom et al., 2017), and WETCHIMP (Melton et al., 2013). The UVic ESCM simulates few CH₄-emitting areas over South-East Asia in comparison to the three model ensembles. The potential underestimation of wetland CH₄ emissions in that region is associated with the relatively few wetland areas simulated by the UVic ESCM (see Section 5.1). In tropical Africa, our model simulates too many CH₄-emitting locations in comparison to the model ensembles (Fig. 10), which is also associated with the distribution

520



of simulated wetlands (see Section 5.1). Nevertheless, the UVic ESCM simulates the occurrence of wetland CH₄ emissions in key source regions such as the Amazon and Congo River basins, South Sudan (Sudd swamps), and Indonesian islands (Fig. 10). For the Amazon and Congo River basins, however, the UVic ESCM simulates lower wetland CH₄ emissions than predicted by the model ensembles (Fig. 10). This can be due to either the consideration of an optimal temperature for CH₄ production (around 27°C) in our model unlike many other process-based models, or the fact that model parameters in this study are tuned to northern estimates.

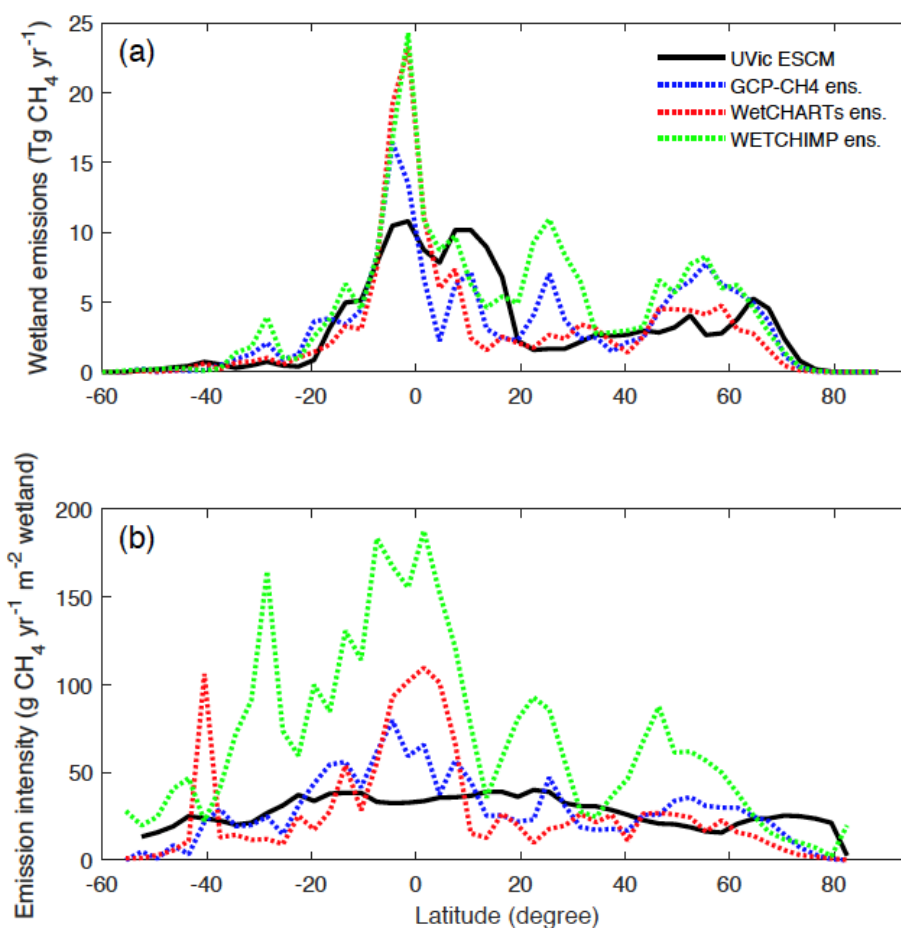


530 **Figure 10: Average methane emissions from global wetlands over the 2001-2004 period as simulated by the UVic ESCM (a) in comparison to three process-based model ensembles: (b) GCP-CH₄, (c) WetCHARTs, and (d) WETCHIMP. The model ensembles are regridded to 3.6° x 1.8° for a fair comparison with the UVic ESCM. The comparison period corresponds to the overlap period for the three model ensembles.**

Fig. 11a shows the latitudinal distribution of simulated wetland CH₄ emissions in comparison to the model ensembles. Interestingly, although GCP-CH₄ and WetCHARTs are based on the same wetland dataset (SWAMPS-GLWD) (Bloom et al., 2017; Poulter et al., 2017), their zonal wetland CH₄ emissions are very different especially near the Equator and across northern high-latitude regions (Fig. 11a).



Using the three model ensembles as reference, the UVic ESCM simulates significantly lower wetland CH₄ emissions around the Equator (Fig. 11a), despite that the model simulates too large equatorial wetland areas (Fig. 4). In fact, wetland emission intensities (emissions per unit of wetland area) by the UVic ESCM are lower than those by the model ensembles between 10°S and 10°N (Fig. 11b) due to relatively large wetland areas but small CH₄ emissions in equatorial regions (Fig. 4 versus Fig. 11a). As previously discussed, the relatively small CH₄ emissions simulated by the UVic ESCM in equatorial regions can be associated with either the optimal temperature for CH₄ production considered in WETMETH but not in most other process-based models, or the fact that model parameters in this study are tuned to northern estimates.



545 **Figure 11: (a) Latitudinal distribution of wetland methane emissions simulated by the UVic ESCM over the 2001-2004 period in comparison to three process-based model ensembles: GCP-CH₄, WetCHARTs and WETCHIMP. The comparison period corresponds to the overlap period for the three model ensembles. (b) Latitudinal emission intensity (methane emissions per unit of wetland area) simulated by the UVic ESCM over the 2001-2004 period in comparison to the three process-based model ensembles. GCP-CH₄ and WetCHARTs both use SWAMPS-GLWD as prescribed wetlands. The wetland methane emissions and emission intensities are summed across latitude bins of 3°.**

550 Furthermore, the UVic ESCM simulates more wetland CH₄ emissions between 10-20°N than the three model ensembles (Fig. 11a) and this can be attributed to the widespread wetlands in West and Central Africa simulated by our



model (Fig. 5 and Fig. 6). In addition, the UVic ESCM simulates significantly less wetland CH₄ emissions between 20-35°N in comparison to the WETCHIMP ensemble (Fig. 11a) and this can be attributed to the relatively small wetland areas simulated by the UVic ESCM in South-East Asia where some models include agricultural wetlands such as rice paddies. Moreover, wetland emission intensities by the UVic ESCM feature low variability with latitude unlike the three model ensembles (Fig. 11b). Such a relative lack of variability can be attributed to two factors: (i) both wetland areas and CH₄ emissions simulated by the UVic ESCM feature relatively low variability with latitude compared to the datasets and model ensembles (Fig. 4 and Fig. 11a); and (ii) as previously discussed, our model likely simulates too large wetland areas but too small CH₄ emissions around the Equator implying a lack of variability across tropical latitudes.

Despite the various discrepancies between the UVic ESCM and both model ensembles regarding the distribution of wetland CH₄ emissions in the tropics, our model simulates mean annual CH₄ emissions from tropical wetlands that are in the range of estimates from the literature (Table 2). For the 1993-2004 period, the UVic ESCM simulates tropical wetland CH₄ emissions of 105.5 Tg CH₄ yr⁻¹ whereas the WETCHIMP ensemble predicts 126 ± 31 Tg CH₄ yr⁻¹ (Melton et al., 2013). Another study suggests a lower mean value (90 ± 77 Tg CH₄ yr⁻¹) for wetland CH₄ emissions in the tropics although with large uncertainties (Sjögersten et al., 2014). Indeed, several studies indicate that wetland CH₄ emissions in the tropics are highly uncertain due to limited ground-based measurements and poorly delimited wetland extent (Dargie et al., 2017; Gumbrecht et al., 2016; Hu et al., 2018; Pangala et al., 2017; Saunois et al., 2020).

6 Model sensitivity to poorly constrained parameters

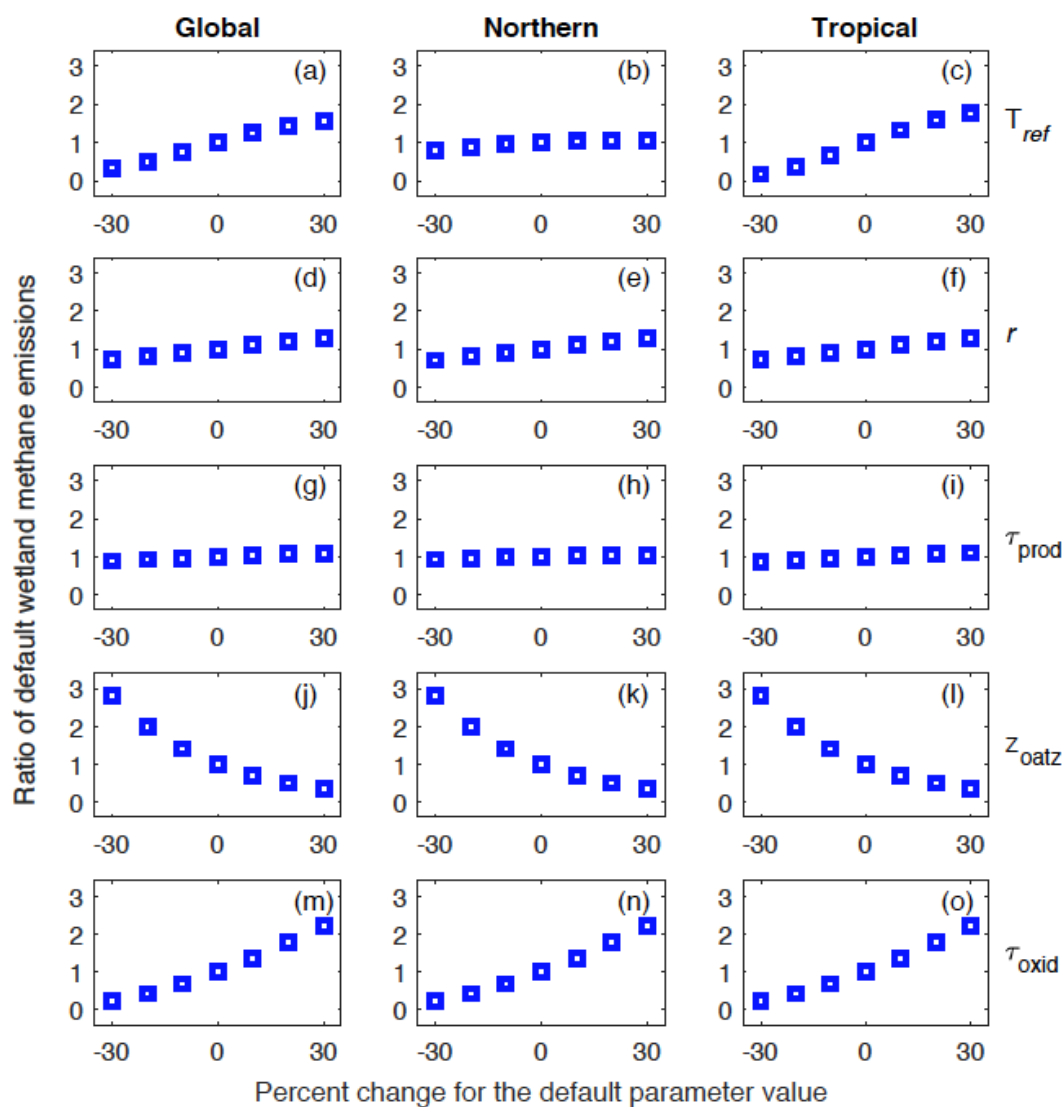
We performed a set of 30 model runs with perturbed parameter values (sensitivity runs) over the 2000-2009 decade in order to analyze the model sensitivity to poorly constrained parameters (T_{ref} , r , τ_{prod} , z_{oatz} , and τ_{oxid}). For each parameter, we increased or decreased the default value by 10, 20, and 30% while holding constant values for other parameters (fixed to default values). We then compared results from the sensitivity runs to the model simulation with all parameter values set to default values (control run). This comparison focuses on the total simulated global (90°S-90°N), northern (45-90°N), and tropical (30°S-30°N) wetland CH₄ emissions over the 2000-2009 decade.

Our results show that the model sensitivity varies with the different parameters and across regions (Fig. 12). Among the five poorly constrained parameters, the UVic ESCM is most sensitive to perturbations of the two parameters for CH₄ oxidation (z_{oatz} and τ_{oxid}) at both the global and regional scale. For z_{oatz} , a decrease (increase) of the default parameter value by 10-30% results in an augmentation (reduction) of default wetland CH₄ emissions by 41-179% (29-64%) at both the global and regional scale (Fig. 12j-l). For τ_{oxid} , a decrease (increase) of the default parameter value by 10-30% implies a reduction (augmentation) of default wetland CH₄ emissions by 32-77% (37-120%) at both the global and regional scale (Fig. 12m-o).

The UVic ESCM is also very sensitive to perturbations of T_{ref} , but this sensitivity is more pronounced for tropical regions than northern regions (Fig. 12a-c). For northern regions, a decrease (increase) of T_{ref} by 10-30% results in a



reduction (augmentation) of default wetland CH₄ emissions by 5-21% (3-5%). For tropical regions, however, a decrease
 585 (increase) of T_{ref} by 10-30% results in a reduction (augmentation) of default wetland CH₄ emissions by 34-82% (33-75%).
 Globally, a decrease (increase) of T_{ref} by 10-30% results in a reduction (augmentation) of default wetland CH₄ emissions by
 26-66% (24-55%). The model sensitivity to perturbations of r is linear across all regions (Fig. 12d-f). Lastly, the model is
 least sensitive to perturbation of τ_{prod} across the globe (Fig. 12g-i).



590 **Figure 12: Analysis of the model sensitivity to perturbations of poorly constrained parameters: T_{ref} , r , τ_{prod} , z_{oatz} , and τ_{oxid} . For each parameter, the default value is increased or decreased by 10, 20, and 30% while values of other parameters are held constant (to default values). The model sensitivity is analyzed with respect to global (90°S-90°N), northern (45-90°N), and tropical (30°S-30°N) wetland methane emissions. Vertical axes show the ratio of the resulting emissions to the default emissions.**



7 Discussions

595 7.1 WETMETH in the spectrum of wetland methane models

A recent study reviewed 40 models of CH₄ emissions in terrestrial ecosystems (predominantly rice paddies and natural wetlands) and classified them into three categories based on their level of complexity: relatively simple models, relatively mechanistic models, and mechanistic models (Xu et al., 2016). Relatively simple models are those that simulate net CH₄ emissions based on soil carbon or other environmental factors without explicit representations for the different CH₄ production and oxidation pathways as well as mechanisms transporting CH₄ to the atmosphere. Relatively mechanistic models are those that account for at least one transport mechanism for CH₄ release in addition to representing CH₄ production and oxidation with simple functions. Mechanistic models are more comprehensive and explicitly simulate different pathways for both CH₄ production and oxidation, more than two mechanisms for CH₄ release, as well as their environmental controls. Based on this classification, WETMETH is a relatively simple model in the sense that it does not distinguish pathways for CH₄ production and oxidation as well as the various mechanisms transporting CH₄ to the atmosphere.

Although some wetland CH₄ models are claimed to be embedded in ESMs (Xu et al., 2016), none of these models are currently run in fully coupled models with feedbacks between climate conditions and the global carbon cycle. Most of these models are rather implemented in dynamic vegetation models or uncoupled land surface components of climate models (Arora et al., 2018; Eliseev et al., 2008; Hodson et al., 2011; Riley et al., 2011; Ringeval et al., 2011; Wania et al., 2009). Nonetheless, relatively simple models present the ideal level of complexity for the current generation of ESMs. More complex models generally imply detailed soil chemistry for O₂ and alternate electron acceptors (Riley et al., 2011; Wania et al., 2010), different carbon substrates and their effects on CH₄ production (Grant, 1998; Lovley and Klug, 1986), an explicit representation of the dynamics of different microbial communities (Grant, 1998; Xu et al., 2015), which all require comprehensive soil chemistry or model parameters that are currently not common in ESMs (Xu et al., 2016). Process parameterizations in mechanistic models generally imply too many degrees of freedom, making it difficult to constrain model parameters against sparse observations. Furthermore, mechanistic models may be too demanding computationally for fully coupled ESM runs without a proportional benefit for large-scale simulations of wetland CH₄ emissions.

The particularity of WETMETH among relatively simple models is that the model accounts for an optimum temperature for CH₄ production, a depth-dependent representation for CH₄ production allowing a calibration of parameters against potential CH₄ production rates from laboratory incubations, dynamic CH₄ oxidation based on the vertical distribution of soil moisture, and the potential for CH₄ emissions in non-inundated ecosystems with relatively high level of soil moisture content. In conclusion, WETMETH is simple enough to be compatible with ESMs and yet complex enough to simulate in an implicit way biogeochemical processes regulating wetland CH₄ emissions.



625 7.2 Limitations for WETMETH

The developed wetland CH₄ model is associated with several limitations, which are linked to either its level of complexity or the scarcity of large-scale datasets for model calibration:

1. The present state of global wetland modelling assumes generic wetlands without distinguishing their different types (Melton et al., 2013; Poulter et al., 2017). Like many other large-scale models of the current generation,
630 WETMETH would not be appropriate for investigating the contribution from particular wetland types to regional or global CH₄ emissions (Aselmann and Crutzen, 1989).
2. Since WETMETH is not based on a comprehensive soil biochemistry module and does not include the different pathways for CH₄ production and oxidation, the model is not suited for investigating the role of specific biological and chemical controls on wetland CH₄ emissions (Bridgman et al., 2013; Kwon et al., 2019).
- 635 3. WETMETH does not simulate the contribution from wetland-specific vegetation species to CH₄ emissions, although some of these species can either lead to high emissions (e.g. sedges are vascular plants that can transport CH₄ through their aerenchyma) or low emissions (e.g. mosses are non-vascular plants that have been shown to develop a symbiotic relationship with methanotrophs) (Bridgman et al., 2013; Chen and Murrell, 2010).
4. Ebullition and aerenchyma of vascular plants allow CH₄ produced in wetlands to escape to the atmosphere with
640 little opportunity for oxidation (Segers, 1998; Whalen, 2005). Moreover, stems of woody trees are important conduits for CH₄ emissions in Amazonia, a major source region in the world (Pangala et al., 2017). By considering the net effect of all mechanisms transporting CH₄ to the atmosphere, WETMETH presents a limitation for investigating the relative contribution of transport mechanisms to CH₄ emissions across regions and at the global scale.
- 645 5. Methane produced in northern wetlands can be stored underneath frozen soil during the winter and be released abruptly upon spring thaw (Mastepanov et al., 2013; Song et al., 2012). WETMETH does not currently feature such a storage of CH₄ in the soil column, which is probably more relevant for small-scale (sites) and short-term (days) than large-scale (regional) and long-term (seasonal) emissions (Fig. 9).
- 650 6. As presented in this study, poorly constrained WETMETH parameters are tuned to estimates from northern high-latitude regions because large-scale datasets from other regions are scarce (see Section 4). A strong limitation comes with the assumption that the chosen parameter values are representative for CH₄ production and oxidation across the globe. However, the applied model calibration remains a reasonable approach given the scarcity of observations for wetland CH₄ production, oxidation, and emissions at the global scale.

Despite these limitations and the model simplicity, WETMETH is skillful when it comes to the simulation of mean seasonal,
655 annual, and decadal wetland CH₄ emissions at the regional, hemispheric, and global scale (see Section 5.2). The implementation of WETMETH in a fully coupled ESM should advance research on the interactions between climate change and wetland CH₄ emissions in the context of global climate projections.



8 Conclusions

This paper introduces WETMETH – a process-based wetland CH₄ model developed for implementation in ESMs. WETMETH is currently embedded in the UVic ESCM, a fully coupled EMIC. WETMETH is a computationally efficient model, applicable globally and, of appropriate complexity with respect to the current state of wetland CH₄ modelling. Unconstrained model parameters are tuned to potential CH₄ production rates from incubated soil samples and CH₄ emissions from northern wetlands due to the scarcity of large-scale datasets from other regions. Nevertheless, WETMETH reproduces well estimates of mean annual CH₄ emissions over the past few decades at the regional, hemispheric, and global scale.

Despite the importance of tropical wetlands in the global CH₄ budget (Kirschke et al., 2013; Saunio et al., 2016) and climate change (O'Connor et al., 2010; Zhang et al., 2017b), their areal extent and associated CH₄ emissions remain highly uncertain in both the literature and modelling work (including this study) due to a combination of limited ground-based measurements and process understanding (Pangala et al., 2017; Saunio et al., 2020; Sjögersten et al., 2014), as well as a low accuracy from remotely-sensed products especially over dense rainforests of Indonesia, Amazonia, and the Congo River basin where new peatlands continue to be discovered to date (Dargie et al., 2017). Large-scale wetland mapping is a field of ongoing research (Tootchi et al., 2019) and further model development should focus on the improvement of wetland simulations in the tropics. In parallel, a compilation of tropical wetland CH₄ measurements from various sources into synthesis datasets would be beneficial for constraining wetland CH₄ processes in large-scale models.

The inclusion of wetland CH₄ processes in a fully coupled ESM allows to advance the research on the feedback between climate change and wetland CH₄ emissions. The implementation of WETMETH in the UVic ESCM constitutes an ideal tool for investigating interactions between climate conditions and wetland CH₄ emissions from decadal to longer timescales. Of particular importance is the permafrost carbon feedback to climate change, in which CH₄ emissions from northern wetlands are expected to play an important role (Nzotungicimpaye and Zickfeld, 2017).



680 **Author contributions**

CMN designed the research under the supervision of KZ, LFWL, JRM, and AHMD. LFWL contributed to the illustrated vertical profiles. CMN developed the wetland methane model with contributions from JRM and KZ. AHMD implemented the TOPMODEL approach in the UVic ESCM to which CMN applied a minor modification. CMN implemented the wetland methane model in the UVic ESCM with contributions from AHMD and ME. CMN performed the model calibration with
685 contributions from CCT and KZ. CMN carried out the model simulations, evaluated the model performance, interpreted the results, and drafted the manuscript. All authors provided critical feedback on the manuscript and helped shape its final version.

Competing interests

The authors declare that they have no conflict of interest.

690 **Code availability**

The code for WETMETH 1.0 embedded in the University of Victoria Earth System Climate Model (UVic ESCM) version 2.9 used in this study is available at <https://doi.org/10.5281/zenodo.4066112> (Nzotungicimpaye and Zickfeld, 2020).

Data availability

WETMETH output variables analyzed in this study are archived at <https://doi.org/10.20383/101.0215> and will be made
695 accessible upon final publication of the manuscript.

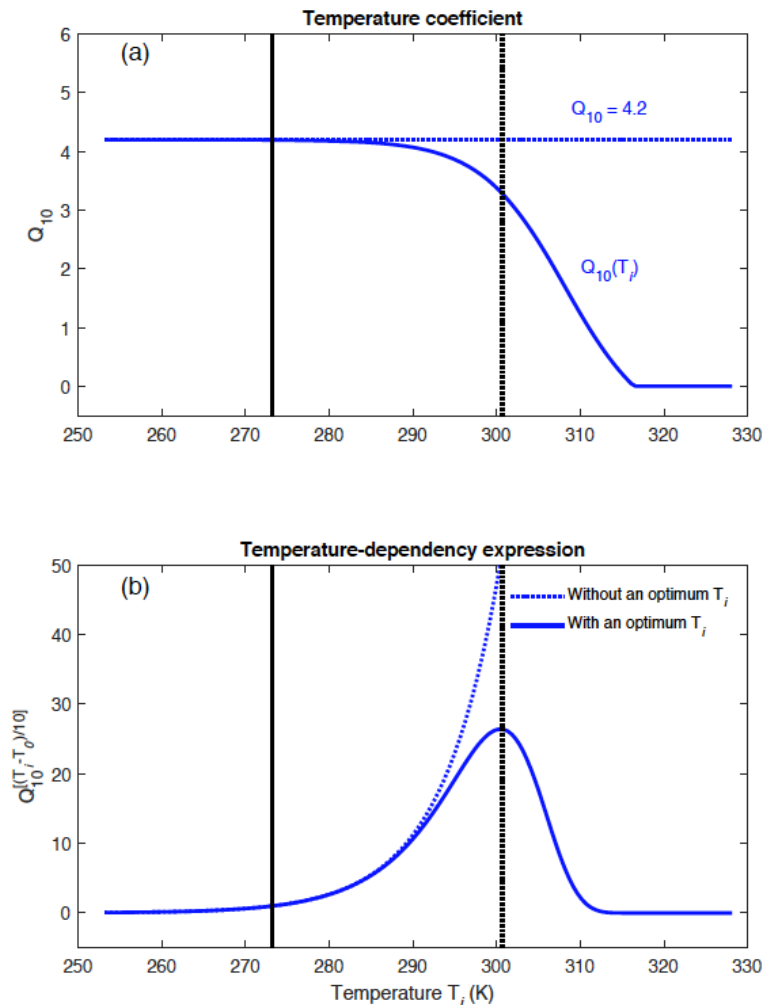
Acknowledgements

KZ and AHMD are each grateful for research funding from the National Sciences and Engineering Research Council of Canada (NSERC) Discovery Grants Program. The authors would like to thank the broad community of researchers who contributed to the datasets and model ensembles used in this study. We thank Catherine Prigent for sharing the GIEMS
700 dataset, and Benjamin Poulter for sharing the SWAMPS-GLWD dataset and the GCP-CH4 model ensemble. We also thank Anthony Bloom, Jed Kaplan, and Olli Peltola for making their methane emission datasets (WetCHARTs ensemble, WETCHIMP ensemble, and the upscaled flux measurements, respectively) publicly available.



Appendix A: Temperature-dependent Q_{10} coefficient for methane production

705 Fig. A1 illustrates the different shapes of the temperature-dependency function for CH_4 production ($Q_{10} \frac{T_i - T_0}{10}$; $T_0 = 273.15$ K) across a range of temperatures when considering: (i) a constant Q_{10} of 4.2; and (ii) a temperature-dependent Q_{10} coefficient given by $Q_{10}(T_i) = 1.7 + 2.5 \tanh [0.1 (T_{ref} - T_i)]$, where $T_{ref} = 308.15$ K. The temperature-dependent $Q_{10}(T_i)$ implies an optimal temperature for CH_4 production in WETMETH around 300.15 K. When $Q_{10}(T_i)$ decreases to reach negative values, its value in WETMETH is set to 10^{-3} to represent a very small methanogenic response to temperature changes (Fig. A1).



710

Figure A1: (a) Differences between a constant Q_{10} coefficient and a temperature-dependent $Q_{10}(T_i)$ coefficients and (b) implications for the temperature-dependency expression for CH_4 production ($Q_{10} \left(\frac{T_i - T_0}{10} \right)$). The temperature-dependent coefficient $Q_{10}(T_i) = 1.7 + 2.5 [\tanh(0.1 (308.15 - T_i))]$ allows to account for uncertainties in the Q_{10} coefficient and to define an optimal temperature for CH_4 production around 300.15 K (dashed vertical line). The freezing point of water is shown at 273.15 K (continuous vertical line).

715



Appendix B: Applied minor modification to the TOPMODEL approach

The TOPMODEL approach implemented in the UVic ESCM is based on the formulation by Gedney and Cox for global land surface models (Gedney and Cox, 2003). This approach combines the simulated hydrology with a prescribed topographic index to determine the occurrence of wetlands (surface inundation) and soil moisture heterogeneity at the sub-grid scale. The occurrence of wetlands is simulated in an area whose local topographic index (Λ) satisfies the following condition:

$$\Lambda_{\min} \leq \Lambda \leq \Lambda_{\max}, \quad (\text{B1})$$

where Λ_{\min} is a lower threshold that can be related to under-saturation conditions and Λ_{\max} is an upper threshold that can be related to over-saturation conditions.

In the initial work by Gedney and Cox, Λ_{\min} depends on the transmissivity of the entire soil column ($T(0)$), the transmissivity of the soil column below the mean water table depth (z_w) of the grid box ($T(z_w)$) as well as the mean topographic index (Λ_{mean}). It is calculated as $\Lambda_{\min} = \ln \frac{T(0)}{T(z_w)} + \Lambda_{\text{mean}}$. While Λ_{mean} is static and prescribed with a topographic index map, both transmissivities ($T(0)$ and $T(z_w)$) are simulated and non-static for a specific grid cell. Hence, Λ_{\min} is a non-static and grid-dependent threshold. Unlike Λ_{\min} , Λ_{\max} is a static and global threshold. This threshold is applied to constrain the occurrence of wetlands in areas of stagnant water based on the assumption that locations where the water table rises well above the surface would be characterized by streamflow.

For the current study, a minor modification is applied to the above TOPMODEL approach. The revision consists of using a non-static and grid-dependent Λ_{\max} instead of a static and global threshold. Following the formulation by Comyn-Platt and colleagues (Comyn-Platt et al., 2018), an expression for Λ_{\max} that depends on Λ_{\min} is currently used in the UVic ESCM. This threshold is defined as:

$$\Lambda_{\max} = \Lambda_{\min} + \Lambda_{\text{range}}, \quad (\text{B2})$$

where Λ_{range} is a global tuning parameter ($\Lambda_{\text{range}} = 0.93$ in the version of the UVic ESCM used in this study).

In summary, unlike the initial work by Gedney and Cox (Gedney and Cox, 2003), the modified TOPMODEL approach considers two non-static and grid-dependent thresholds (Λ_{\min} and Λ_{\max}) for the identification of wetlands across the globe.

Appendix C: Unit conversion for potential methane production rates

Here, we describe steps followed for converting units of maximum CH_4 production rates measured in laboratory incubations from a soil weight basis ($\mu\text{g C g DW}^{-1} \text{ hr}^{-1}$) to a soil volume basis ($\text{kg C m}^{-3} \text{ s}^{-1}$). This unit conversion relies on the soil bulk density (BD in g cm^{-3}) from the site of origin. The following two steps illustrate the applied unit conversion. In the first step, the potential CH_4 production rates ($P_{d,0}$) are converted from $\mu\text{g C g DW}^{-1} \text{ hr}^{-1}$ to $\mu\text{g C cm}^{-3} \text{ hr}^{-1}$ as follows:

$$P_{d,1} = (\text{BD}) P_{d,0} \quad (\text{C1})$$

Then, the conversion of $P_{d,1}$ from $\mu\text{g C cm}^{-3} \text{ hr}^{-1}$ to $\text{kg C m}^{-3} \text{ s}^{-1}$ is done as follows:



$$P_{d,2} = \frac{\delta}{\gamma} P_{d,1}, \quad (C2)$$

where δ encompasses the conversion factors from μg to kg and from cm^{-3} to m^{-3} ($\delta = 10^{-3} \text{ kg m}^{-3}$); and γ is the number of seconds per hour ($\gamma = 3600 \text{ s}$).



750 References

- Archer, D.: A data-driven model of the global calcite lysocline, *Global Biogeochem. Cycles*, 10, 511–526, 1996.
- Arora, V. K., Boer, G. J., Friedlingstein, P., Eby, M., Jones, C. D., Christian, J. R., Bonan, G., Bopp, L., Brovkin, V., Cadule, P., Hajima, T., Ilyina, T., Lindsay, K., Tjiputra, J. F. and Wu, T.: Carbon-concentration and carbon-climate feedbacks in CMIP5 earth system models, *J. Clim.*, 26, 5289–5314, 2013.
- 755 Arora, V. K., Melton, J. R. and Plummer, D.: An assessment of natural methane fluxes simulated by the CLASS-CTEM model, *Biogeosciences*, 15, 4683–4709, 2018.
- Aselmann, I. and Crutzen, P. J.: Global distribution of natural freshwater wetlands and rice paddies, their net primary productivity, seasonality and possible methane emissions, *J. Atmos. Chem.*, 8, 307–358, 1989.
- Avis, C. A., Weaver, A. J. and Meissner, K. J.: Reduction in areal extent of high-latitude wetlands in response to permafrost thaw, *Nat. Geosci.*, 4, 444–448, 2011.
- 760 Barba, J., Bradford, M., Brewer, P., Bruhn, D., Covey, K., von Haren, J., Megonigal, J., Mikkelsen, T., Pangala, S., Pihlatie, M., Poulter, B., Rivas-Ubach, A., Schadt, C., Terazawa, K., Warner, D., Zhang, Z. and Vargas, R.: Methane emissions from tree stems: a new frontier in the global carbon cycle, *New Phytol.*, 222, 18–28, 2019.
- Blake, L. I., Tveit, A., Øvreås, L., Head, I. M. and Gray, N. D.: Response of methanogens in arctic sediments to temperature and methanogenic substrate availability, *PLoS One*, 10, 1–18, 2015.
- 765 Blazewicz, S. J., Petersen, D. G., Waldrop, M. P. and Firestone, M. K.: Anaerobic oxidation of methane in tropical and boreal soils: Ecological significance in terrestrial methane cycling, *J. Geophys. Res. Biogeosciences*, 117, 1–9, 2012.
- Blodau, C.: Carbon cycling in peatlands - A review of processes and controls, *Environ. Rev.*, 10, 111–134, 2002.
- Blodau, C., Basiliko, N. and Moore, T. R.: Carbon turnover in peatland mesocosms exposed to different water table levels, *Biogeochemistry*, 67, 331–351, 2004.
- 770 Bloom, A. A., Bowman, K. W., Lee, M., Turner, A. J., Schroeder, R., Worden, J. R., Weidner, R., McDonald, K. C. and Jacob, D. J.: A global wetland methane emissions and uncertainty dataset for atmospheric chemical transport models (WetCHARTs version 1.0), *Geosci. Model Dev.*, 10, 2141–2156, 2017.
- Bohn, T. J., Melton, J. R., Ito, A., Kleinen, T., Spahni, R., Stocker, B. D., Zhang, B., Zhu, X., Schroeder, R., Glagolev, M. V., Maksyutov, S., Brovkin, V., Chen, G., Denisov, S. N., Eliseev, A. V., Gallego-Sala, A., McDonald, K. C., Rawlins, M. A., Riley, W. J., Subin, Z. M., Tian, H., Zhuang, Q. and Kaplan, J. O.: WETCHIMP-WSL: Intercomparison of wetland methane emissions models over West Siberia, *Biogeosciences*, 12, 3321–3349, 2015.
- 775 Bridgman, S. D., Cadillo-Quiroz, H., Keller, J. K. and Zhuang, Q.: Methane emissions from wetlands: biogeochemical, microbial, and modeling perspectives from local to global scales, *Glob. Chang. Biol.*, 19, 1325–1346, 2013.
- 780 Brune, A., Frenzel, P. and Cypionka, H.: Life at the oxic-anoxic interface: microbial activities and adaptations, *FEMS Microbiol. Rev.*, 24, 691–710, 2000.
- Cadillo-Quiroz, H., Bräuer, S., Yashiro, E., Sun, C., Yavitt, J. and Zinder, S.: Vertical profiles of methanogenesis and methanogens in two contrasting acidic peatlands in central New York State, USA, *Environ. Microbiol.*, 8, 1428–1440, 2006.
- 785 Chen, Y. and Murrell, J. C.: Methanotrophs in moss, *Nature*, 3, 595–596, 2010.
- Comyn-Platt, E., Hayman, G., Huntingford, C., Chadburn, S. E., Burke, E. J., Harper, A. B., Collins, W. J., Webber, C. P., Powell, T., Cox, P. M., Gedney, N. and Sitch, S.: Carbon budgets for 1.5 and 2°C targets lowered by natural wetland and permafrost feedbacks, *Nat. Geosci.*, 11, 568–573, 2018.
- Conrad, R.: The global methane cycle: Recent advances in understanding the microbial processes involved, *Environ. Microbiol. Rep.*, 1, 285–292, 2009.
- 790 Couwenberg, J., Dommain, R. and Joosten, H.: Greenhouse gas fluxes from tropical peatlands in south-east Asia, *Glob. Chang. Biol.*, 16, 1715–1732, 2010.
- Cox, P. M.: Description of the TRIFFID Dynamic Global Vegetation Model, Exeter, UK., 2001.
- Dargie, G. C., Lewis, S. L., Lawson, I. T., Mitchard, E. T. A., Page, S. E., Bocko, Y. E. and Ifo, S. A.: Age, extent and carbon storage of the central Congo Basin peatland complex, *Nature*, 542, 86–90, 2017.
- 795 Dean, J. F., Middelburg, J. J., Röckmann, T., Aerts, R., Blauw, L. G., Egger, M., Jetten, M. S. M., de Jong, A. E. E., Meisel, O. H., Rasigraf, O., Slomp, C. P., in't Zandt, M. and Dolman, A. J.: Methane feedbacks to the global climate system in a warmer world, *Rev. Geophys.*, 56, 207–250, 2018.



- 800 Dunfield, P., Knowles, R., Dumont, R. and Moore, T. R.: Methane production and consumption in temperate and subarctic peat soils: Response to temperature and pH, *Soil Biol. Biogeochem.*, 25, 321–326, 1993.
- Duval, T. and Radu, D.: Effect of temperature and soil organic matter quality on greenhouse gas production from temperate poor and rich fen soils, *Ecol. Eng.*, 114, 167–172, 2018.
- Eby, M., Zickfeld, K., Montenegro, A., Archer, D., Meissner, K. J. and Weaver, A. J.: Lifetime of anthropogenic climate change: Millennial time scales of potential CO₂ and surface temperature perturbations, *J. Clim.*, 22, 2501–2511, 2009.
- 805 Eliseev, A. V., Mokhov, I. I., Arzhanov, M. M., Demchenko, P. F. and Denisov, S. N.: Interaction of the methane cycle and processes in wetland ecosystems in a climate model of intermediate complexity, *Atmos. Ocean. Phys.*, 44, 147–162, 2008.
- Estop-Aragonés, C., Knorr, K.-H. and Blodau, C.: Controls on in situ oxygen and dissolved inorganic carbon dynamics in peats of a temperate fen, *J. Geophys. Res.*, 117, G02002, 2012.
- 810 Frolking, S., Roulet, N. T., Moore, T. R., Lafleur, P. M., Bubier, J. L. and Crill, P. M.: Modeling seasonal to annual carbon balance of Mer Bleue Bog, Ontario, Canada, *Global Biogeochem. Cycles*, 16, 1–21, 2002.
- Gauthier, M., Bradley, R. and Šimek, M.: More evidence that anaerobic oxidation of methane is prevalent in soils: Is it time to upgrade our biogeochemical models?, *Soil Biol. Biochem.*, 80, 167–174, 2015.
- Gedney, N. and Cox, P. M.: The sensitivity of global climate model simulations to the representation of soil moisture heterogeneity, *J. Hydrometeorol.*, 4, 1265–1275, 2003.
- 815 Gedney, N., Cox, P. M. and Huntingford, C.: Climate feedback from wetland methane emissions, *Geophys. Res. Lett.*, 31, L20503, 2004.
- Gedney, N., Huntingford, C., Comyn-Platt, E. and Wiltshire, A.: Significant feedbacks of wetland methane release on climate change and the causes of their uncertainty, *Environ. Res. Lett.*, 14, 084027, 2019.
- 820 Girkin, N. T., Turner, B. L., Ostle, N., Craigan, J. and Sjögersten, S.: Root exudate analogues accelerate CO₂ and CH₄ production in tropical peat, *Soil Biol. Biochem.*, 117, 48–55, 2018.
- Glagolev, M., Kleptsova, I., Filippov, I., Maksyutov, S. and Machida, T.: Regional methane emission from West Siberia mire landscapes, *Environ. Res. Lett.*, 6, 045214, 2011.
- Grant, R. F.: Simulation of methanogenesis in the mathematical model ecosys, *Soil Biol. Biochem.*, 30, 883–896, 1998.
- 825 Gumbrecht, T., Roman-Cuesta, R., Verchot, L., Herold, M., Wittmann, F., Householder, E., Herold, N. and Murdiyarso, D.: An expert system model for mapping tropical wetlands and peatlands reveals South America as the largest contributor, *Glob. Chang. Biol.*, 23, 3581–3599, 2016.
- Hegarty, T.: Temperature coefficient (Q₁₀), seed germination and other biological processes, *Nature*, (243), 305–306, 1973.
- 830 Helbig, M., Quinton, W. L. and Sonnentag, O.: Warmer spring conditions increase annual methane emissions from a boreal peat landscape with sporadic permafrost, *Environ. Res. Lett.*, 12, 115009, 2017.
- Hodson, E. L., Poulter, B., Zimmermann, N. E., Prigent, C. and Kaplan, J. O.: The El Niño-Southern Oscillation and wetland methane interannual variability, *Geophys. Res. Lett.*, 38, L08810, 2011.
- Hoehler, T. and Alperin, M.: Methane minimalism, *Nature*, 507, 436–437, 2014.
- 835 Hoehler, T. M., Alperin, M. J., Albert, D. B. and Martens, C. S.: Field and laboratory studies of methane oxidation in an anoxic marine sediment: Evidence for a methanogen-sulfate reducer consortium, *Global Biogeochem. Cycles*, 8, 451–463, 1994.
- Hopcroft, P. O., Valdes, P. J. and Beerling, D. J.: Simulating idealized Dansgaard-Oeschger events and their potential impacts on the global methane cycle, *Quat. Sci. Rev.*, 30, 3258–3268, 2011.
- 840 Hu, H., Landgraf, J., Detmers, R., Borsdorff, T., Aan de Brugh, J., Aben, I., Butz, A. and Hasekamp, O.: Toward global mapping of methane with TROPOMI: First results and intersatellite comparison to GOSAT, *Geophys. Res. Lett.*, 45, 3682–3689, 2018.
- Jauhiainen, J., Takahashi, H., Heikkinen, J. E. P., Martikainen, P. J. and Vasander, H.: Carbon fluxes from a tropical peat swamp forest floor, *Glob. Chang. Biol.*, 11, 1788–1797, 2005.
- 845 Kim, Y.: Effect of thaw depth on fluxes of CO₂ and CH₄ in manipulated Arctic coastal tundra of Barrow, Alaska, *Sci. Total Environ.*, 505, 385–389, 2015.
- Kirschke, S., Bousquet, P., Ciais, P., Saunois, M., Canadell, J. G., Dlugokencky, E. J., Bergamaschi, P., Bergmann, D., Blake, D. R., Bruhwiler, L., Cameron-Smith, P., Castaldi, S., Chevallier, F., Feng, L., Fraser, A., Heimann, M., Hodson, E. L., Houweling, S., Josse, B., Fraser, P. J., Krummel, P. B., Lamarque, J.-F., Langenfelds, R. L., Le Quééré, C., Naik,



- 850 V., Palmer, P. I., Pison, I., Plummer, D., Poulter, B., Prinn, R. G., Rigby, M., Ringeval, B., Santini, M., Schmidt, M.,
Shindell, D. T., Simpson, I. J., Spahni, R., Paul Steele, L., Strode, S. A., Sudo, K., Szopa, S., Van der Werf, G. R.,
Voulgarakis, A., Van Weele, M., Weiss, R. F., Williams, J. E. and Zeng, G.: Three decades of global methane sources
and sinks, *Nat. Geosci.*, 6, 813–823, 2013.
- 855 Koven, C. D., Ringeval, B., Friedlingstein, P., Ciais, P., Cadule, P., Khvorostyanov, D., Krinner, G. and Tarnocai, C.:
Permafrost carbon-climate feedbacks accelerate global warming, *Proc. Natl. Acad. Sci. U. S. A.*, 108, 14769–14774,
2011.
- Koven, C. D., Lawrence, D. M. and Riley, W. J.: Permafrost carbon–climate feedback is sensitive to deep soil carbon
decomposability but not deep soil nitrogen dynamics, *Proc. Natl. Acad. Sci. U. S. A.*, 112, 3752–3757, 2015.
- Kwon, M., Jung, J., Tripathi, B., Göckede, M., Lee, Y. and Kim, M.: Dynamics of microbial communities and CO₂ and CH₄
fluxes in the tundra ecosystems of the changing Arctic, *J. Microbiol.*, 57, 325–336, 2019.
- 860 Loulergue, L., Schilt, A., Spahni, R., Masson-Delmotte, V., Blunier, T., Lemieux, B., Barnola, J., Raynaud, D., Stocker, T.
and Chappellaz, J.: Orbital and millennial-scale features of atmospheric CH₄ over the past 800,000 years, *Nature*, 453,
383–386, 2008.
- Lovley, D. R. and Klug, M. J.: Model for the distribution of sulfate reduction and methanogenesis in freshwater sediments,
Geochim. Cosmochim. Acta, 50, 11–18, 1986.
- 865 Lupascu, M., Wadham, E. R. C. and Pancost, R. D.: Temperature sensitivity of methane production in the permafrost active
layer at Stordalen, Sweden: A comparison with non-permafrost northern wetlands, *Arctic, Antarct. Alp. Res.*, 44, 469–
482, 2012.
- MacDougall, A. H. and Knutti, R.: Projecting the release of carbon from permafrost soils using a perturbed parameter
ensemble modelling approach, *Biogeosciences*, 13, 2123–2136, 2016.
- 870 MacDougall, A. H., Avis, C. A. and Weaver, A. J.: Significant contribution to climate warming from the permafrost carbon
feedback, *Nat. Geosci.*, 5, 719–721, 2012.
- Mastepanov, M., Sigsgaard, C., Tagesson, T., Ström, L., Tamstorf, M. P., Lund, M. and Christensen, T. R.: Revisiting
factors controlling methane emissions from high-Arctic tundra, *Biogeosciences*, 10, 5139–5158, 2013.
- 875 Matthews, H. D., Weaver, A. J., Meissner, K. J., Gillett, N. P. and Eby, M.: Natural and anthropogenic climate change:
Incorporating historical land cover change, vegetation dynamics and the global carbon cycle, *Clim. Dyn.*, 22, 461–479,
2004.
- McCalley, C. K., Woodcroft, B. J., Hodgkins, S. B., Wehr, R. A., Kim, E.-H., Mondav, R., Crill, P. M., Chanton, J. P., Rich,
V. I., Tyson, G. W. and Saleska, S. R.: Methane dynamics regulated by microbial community response to permafrost
thaw, *Nature*, 514, 478–481, 2014.
- 880 Meissner, K. J., Weaver, A. J., Matthews, H. D. and Cox, P. M.: The role of land surface dynamics in glacial inception: A
study with the UVic Earth System Model, *Clim. Dyn.*, 21, 515–537, 2003.
- Melton, J. R., Wania, R., Hodson, E. L., Poulter, B., Ringeval, B., Spahni, R., Bohn, T., Avis, C. A., Beerling, D. J., Chen,
G., Eliseev, A. V., Denisov, S. N., Hopcroft, P. O., Lettenmaier, D. P., Riley, W. J., Singarayer, J. S., Subin, Z. M., Tian,
H., Zürcher, S., Brovkin, V., Van Bodegom, P. M., Kleinen, T., Yu, Z. C. and Kaplan, J. O.: Present state of global
885 wetland extent and wetland methane modelling: Conclusions from a model inter-comparison project (WETCHIMP),
Biogeosciences, 10, 753–788, 2013.
- Le Mer, J. and Roger, P.: Production, oxidation, emission and consumption of methane by soils: A review, *Eur. J. Soil Biol.*,
37, 25–50, 2001.
- 890 Miller, S. M., Worthy, D. E. J., Michalak, A. M., Wofsy, S. C., Kort, E. A., Havice, T. C., Andrews, A. E., Dlugokencky, E.
J., Kaplan, J. O., Levi, P. J., Tian, H. and Zhang, B.: Observational constraints on the distribution, seasonality, and
environmental predictors of North American boreal methane emissions, *Global Biogeochem. Cycles*, 28, 146–160, 2014.
- Mitsch, W. and Mander, Ü.: Wetlands and carbon revisited, *Ecol. Eng.*, 114, 1–6, 2018.
- Moore, T. and Roulet, N.: Methane flux: Water table relations in northern wetlands, *Geophys. Res. Lett.*, 20, 587–590, 1993.
- 895 Moosavi, S. and Crill, P.: CH₄ oxidation by tundra wetlands as measured by a selective inhibitor technique, *J. Geophys. Res.*
Atmos., 103, 29093–29106, 1998.
- Nzotungicimpaye, C.-M. and Zickfeld, K.: The contribution from methane to the permafrost carbon feedback, *Curr. Clim.*
Chang. Reports, 3, 58–68, 2017.



- 900 Nzotungicimpaye, C.-M. and Zickfeld, K.: The first version of WETMETH, a model for wetland methane emissions (WETMETH 1.0), Zenodo, doi:<https://doi.org/10.5281/zenodo.4066112>, 2020.
- O'Connor, F. M., Boucher, O., Gedney, N., Jones, C. D., Folberth, G. A., Coppell, R., Friedlingstein, P., Collins, W. J., Chappellaz, J., Ridley, J. and Johnson, C. E.: Possible role of wetlands, permafrost, and methane hydrates in the methane cycle under future climate change: A review, *Rev. Geophys.*, 48, RG4005, 2010.
- 905 Olefeldt, D., Turetsky, M. R., Crill, P. M. and McGuire, A. D.: Environmental and physical controls on northern terrestrial methane emissions across permafrost zones, *Glob. Chang. Biol.*, 19, 589–603, 2013.
- Orr, J. C.: On ocean carbon-cycle model comparison, *Tellus B*, 51, 509–510, 1999.
- Pandey, S., Houweling, S., Krol, M., Aben, I., Monteil, G., Nechita-Banda, N., Dlugokencky, E. J., Detmers, R., Hasekamp, O., Xu, X., Riley, W. J., Poulter, B., Zhang, Z., McDonald, K. C., White, J. W. C., Bousquet, P. and Röckmann, T.: Enhanced methane emissions from tropical wetlands during the 2011 La Niña, *Sci. Rep.*, 7, 45759, 2017.
- 910 Pangala, S. R., Enrich-Prast, A., Basso, L. S., Peixoto, R. B., Bastviken, D., Hornibrook, E. R. C., Gatti, L. V., Ribeiro, H., Calazans, L. S. B., Sakuragui, C. M., Bastos, W. R., Malm, O., Gloor, E., Miller, J. B. and Gauci, V.: Large emissions from floodplains trees close the Amazon methane budget, *Nature*, 522, 230–234, 2017.
- Panikov, N. S. and Dedysh, S. N.: Cold season CH₄ and CO₂ emission from boreal peat bogs (West Siberia): Winter fluxes and thaw activation dynamics, *Global Biogeochem. Cycles*, 14, 1071–1080, 2000.
- 915 Papa, F., Prigent, C., Aires, F., Jimenez, C., Rossow, W. B. and Matthews, E.: Interannual variability of surface water extent at the global scale, 1993-2004, *J. Geophys. Res. Atmos.*, 115, D12111, 2010.
- Paudel, R., Mahowald, N. M., Hess, P. G. M., Meng, L. and Riley, W. J.: Attribution of changes in global wetland methane emissions from pre-industrial to present using CLM4.5-BGC, *Environ. Res. Lett.*, 11, 034020, 2016.
- 920 Peltola, O., Vesala, T., Gao, Y., Rätty, O., Alekseychik, P., Aurela, M., Chojnicki, B., Desai, A. R., Dolman, A. J., Euskirchen, E. S., Friborg, T., Göckede, M., Helbig, M., Humphreys, E., Jackson, R. B., Jocher, G., Joos, F., Klatt, J., Knox, S. H., Kowalska, N., Kutzbach, L., Lienert, S., Lohila, A., Mammarella, I., Nadeau, D. F., Nilsson, M. B., Oechel, W. C., Peichl, M., Pypker, T., Quinton, W., Rinne, J., Sachs, T., Samson, M., Schmid, H. P., Sonnentag, O., Wille, C., Zona, D. and Aalto, T.: Monthly gridded data product of northern wetland methane emissions based on upscaling eddy covariance observations, *Earth Syst. Sci. Data*, 11, 1263–1289, 2019.
- 925 Pickett-Heaps, C. A., Jacob, D. J., Wecht, K. J., Kort, E. A., Wofsy, S. C., Diskin, G. S., Worthy, D. E. ., Kaplan, J. O., Bey, I. and Drevet, J.: Magnitude and seasonality of wetland methane emissions from the Hudson Bay Lowlands (Canada), *Atmos. Chem. Phys.*, 11, 3773–3779, 2011.
- Poindexter, C. M., Baldocchi, D. D., Matthes, J. H., Knox, S. H. and Variano, E. A.: The contribution of an overlooked transport process to a wetland's methane emissions, *Geophys. Res. Lett.*, 43, 6276–6284, 2016.
- 930 Poulter, B., Bousquet, P., Canadell, J. G., Ciais, P., Peregon, A., Saunois, M., Arora, V. K., Beerling, D. J., Brovkin, V., Jones, C. D., Joos, F., Gedney, N., Ito, A., Kleinen, T., Koven, C. D., McDonald, K., Melton, J. R., Peng, C., Peng, S., Prigent, C., Schroeder, R., Riley, W. J., Saito, M., Spahni, R., Tian, H., Taylor, L., Viovy, N., Wilton, D., Wiltshire, A., Xu, X., Zhang, B., Zhang, Z. and Zhu, Q.: Global wetland contribution to 2000-2012 atmospheric methane growth rate dynamics, *Environ. Res. Lett.*, 12, 094013, 2017.
- 935 Prigent, C., Matthews, E., Aires, F. and Rossow, W. B.: Remote sensing of global wetland dynamics with multiple satellite data sets, *Geophys. Res. Lett.*, 28, 4631–4634, 2001.
- Prigent, C., Papa, F., Aires, F., Rossow, W. B. and Matthews, E.: Global inundation dynamics inferred from multiple satellite observations, 1993-2000, *J. Geophys. Res. Atmos.*, 112, D12107, 2007.
- 940 Prigent, C., Papa, F., Aires, F., Jiménez, C., Rossow, W. B. and Matthews, E.: Changes in land surface water dynamics since the 1990s and relation to population pressure, *Geophys. Res. Lett.*, 39, L08403, 2012.
- Reeburgh, W.: Methane consumption in Cariaco Trench waters and sediments, *Earth Planet. Sci. Lett.*, 28, 337–344, 1976.
- Rhodes, R. H., Brook, E. J., McConnell, J. R., Blunier, T., Sime, L. C., Faïn, X. and Mulvaney, R.: Atmospheric methane variability: Centennial-scale signals in the Last Glacial Period, *Global Biogeochem. Cycles*, 31, 575–590, 2017.
- 945 Riley, W. J., Subin, Z. M., Lawrence, D. M., Swenson, S. C., Torn, M. S., Meng, L., Mahowald, N. M. and Hess, P.: Barriers to predicting changes in global terrestrial methane fluxes: Analyses using CLM4Me, a methane biogeochemistry model integrated in CESM, *Biogeosciences*, 8, 1925–1953, 2011.
- Ringeval, B., Friedlingstein, P., Koven, C., Ciais, P., De Noblet-Ducoudré, N., Decharme, B. and Cadule, P.: Climate-CH₄ feedback from wetlands and its interaction with the climate-CO₂ feedback, *Biogeosciences*, 8, 2137–2157, 2011.



- 950 Rivkina, E., Laurinavichius, K., McGrath, J., Tiedje, J., Shcherbakova, V. and Gilichinsky, D.: Microbial life in permafrost, *Adv. Sp. Res.*, 33, 1215–1221, 2004.
- Rogelj, J., Forster, P. M., Kriegler, E., Smith, C. J. and Séférian, R.: Estimating and tracking the remaining carbon budget for stringent climate targets, *Nature*, 571, 335–342, 2019.
- Roslev, P. and King, G.: Regulation of methane oxidation in a freshwater wetland by water table changes and anoxia, *FEMS Microbiol. Ecol.*, 19, 105–115, 1996.
- 955 Saunio, M., Bousquet, P., Poulter, B., Peregon, A., Ciais, P., Canadell, J. G., Dlugokencky, E. J., Etiope, G., Bastviken, D., Houweling, S., Mcdonald, K. C., Marshall, J., Melton, J. R., Morino, I., Naik, V., O’Doherty, S., Parmentier, F.-J. W., Patra, P. K., Peng, C., Peng, S., Peters, G. P., Pison, I., Prigent, C., Prinn, R., Ramonet, M., Riley, W. J., Saito, M., Santini, M., Schroeder, R., Simpson, I. J., Spahni, R., Steele, P., Takizawa, A., Thornton, B. F., Tian, H., Tohjima, Y., Viovy, N., Voulgarakis, A., Van Weele, M., Van Der Werf, G. R., Weiss, R., Wiedinmyer, C., Wilton, D. J., Wiltshire, 960 A., Worthy, D., Wunch, D., Xu, X., Yoshida, Y., Zhang, B., Zhang, Z. and Zhu, Q.: The global methane budget 2000–2012, *Earth Syst. Sci. Data*, 8, 697–751, 2016.
- Saunio, M., Stavert, A. R., Poulter, B., Bousquet, P., Canadell, J. G., Jackson, R. B., Raymond, P. A., Dlugokencky, E. J., Houweling, S., Patra, P. K., Ciais, P., Arora, V. K., Bastviken, D., Bergamaschi, P., Blake, D. R., Brailsford, G., Bruhwiler, L., Carlson, K. M., Carrol, M., Castaldi, S., Chandra, N., Crevoisier, C., Crill, P. M., Covey, K., Curry, C. L., 965 Etiope, G., Frankenberg, C., Gedney, N., Hegglin, M. I., Höglund-Isaksson, L., Hugelius, G., Ishizawa, M., Ito, A., Janssens-Maenhout, G., Jensen, K. M., Joos, F., Kleinen, T., Krummel, P. B., Langenfelds, R. L., Laruelle, G. G., Liu, L., Machida, T., Maksyutov, S., McDonald, K. C., McNorton, J., Miller, P. A., Melton, J. R., Morino, I., Müller, J., Murguia-Flores, F., Naik, V., Niwa, Y., Noce, S., O’Doherty, S., Parker, R. J., Peng, C., Peng, S., Peters, G. P., Prigent, C., Prinn, R., Ramonet, M., Regnier, P., Riley, W. J., Rosentreter, J. A., Segers, A., Simpson, I. J., Shi, H., Smith, S. J., 970 Steele, L. P., Thornton, B. F., Tian, H., Tohjima, Y., Tubiello, F. N., Tsuruta, A., Viovy, N., Voulgarakis, A., Weber, T. S., Van Weele, M., Van der Werf, G. R., Weiss, R. F., Worthy, D., Wunch, D., Yin, Y., Yoshida, Y., Zhang, W., Zhang, Z., Zhao, Y., Zheng, B., Zhu, Q., Zhu, Q. and Zhuang, Q.: The global methane budget 2000–2017, *Earth Syst. Sci. Data*, 12, 1561–1623, 2020.
- Schmittner, A., Oschlies, A., Matthews, H. D. and Galbraith, E. D.: Future changes in climate, ocean circulation, ecosystems, and biogeochemical cycling simulated for a business-as-usual CO₂ emission scenario until year 4000 AD, *Global Biogeochem. Cycles*, 22, GB1013, 2008.
- Schneider von Deimling, T., Meinshausen, M., Levermann, A., Huber, V., Frieler, K., Lawrence, D. M. and Brovkin, V.: Estimating the near-surface permafrost-carbon feedback on global warming, *Biogeosciences*, 9, 649–665, 2012.
- Schneider von Deimling, T., Grosse, G., Strauss, J., Schirrmeyer, L., Morgenstern, A., Schaphoff, S., Meinshausen, M. and 980 Boike, J.: Observation-based modelling of permafrost carbon fluxes with accounting for deep carbon deposits and thermokarst activity, *Biogeosciences*, 12, 3469–3488, 2015.
- Schuur, E. A. G., McGuire, A. D., Schädel, C., Grosse, G., Harden, J. W., Hayes, D. J., Hugelius, G., Koven, C. D., Kuhry, P., Lawrence, D. M., Natali, S. M., Olefeldt, D., Romanovsky, V. E., Schaefer, K., Turetsky, M. R., Treat, C. C. and Vonk, J. E.: Climate change and the permafrost carbon feedback, *Nature*, 520, 171–179, 2015.
- 985 Segers, R.: Methane production and methane consumption: A review of processes underlying wetland methane fluxes, *Biogeochemistry*, 41, 23–51, 1998.
- Shindell, D. T., Walter, B. P. and Faluvegi, G.: Impacts of climate change on methane emissions from wetlands, *Geophys. Res. Lett.*, 31, L21202, 2004.
- Singleton, C. M., McCalley, C. K., Woodcroft, B. J., Boyd, J. A., Evans, P. N., Hodgkins, S. B., Chanton, J. P., Froelking, S., 990 Crill, P. M., Saleska, S. R., Rich, V. I. and Tyson, G. W.: Methanotrophy across a natural permafrost thaw environment, *ISME J.*, 12, 2544–2558, 2018.
- Sjögersten, S., Black, C., Evers, S., Hoyos-Santillan, J., Wright, E. and Turner, B.: Tropical wetlands: A missing link in the global carbon cycle?, *Global Biogeochem. Cycles*, 28, 1371–1386, 2014.
- Sjögersten, S., Aplin, P., Gauci, V., Peacock, M., Siegenthaler, A. and Turner, B. L.: Temperature response of ex-situ greenhouse gas emissions from tropical peatlands: Interactions between forest type and peat moisture conditions, *Geoderma*, 324, 47–55, 2018.
- 995 Smemo, K. A. and Yavitt, J. B.: Anaerobic oxidation of methane: An underappreciated aspect of methane cycling in peatland ecosystems?, *Biogeosciences*, 8, 779–793, 2011.



- 1000 Song, C., Xu, X., Sun, X., Tian, H., Sun, L., Miao, Y., Wang, X. and Guo, Y.: Large methane emission upon spring thaw from natural wetlands in the northern permafrost region, *Environ. Res. Lett.*, 7, 034009, 2012.
- Taylor, K. E., Stouffer, R. J. and Meehl, G. A.: An overview of CMIP5 and the experiment design, *Bull. Am. Meteorol. Soc.*, 93, 485–498, 2012.
- 1005 Thompson, R. L., Sasakawa, M., Machida, T., Aalto, T., Worthy, D., Lavric, J. V., Myhre, C. L. and Stohl, A.: Methane fluxes in the high northern latitudes for 2005–2013 estimated using a Bayesian atmospheric inversion, *Atmos. Chem. Phys.*, 17, 3553–3572, 2017.
- Thornton, B., Wik, M. and Crill, P. M.: Double-counting challenges the accuracy of high-latitude methane inventories, *Geophys. Res. Lett.*, 43, 12569–12577, 2016.
- Tokarska, K. and Gillett, N.: Cumulative carbon emissions budgets consistent with 1.5°C global warming, *Nat. Clim. Chang.*, 8, 296–299, 2018.
- 1010 Tootchi, A., Jost, A. and Ducharne, A.: Multi-source global wetland maps combining surface water imagery and groundwater constraints, *Earth Syst. Sci. Data*, 11, 189–220, 2019.
- Treat, C. C., Natali, S. M., Ernakovich, J., Iversen, C. M., Lupascu, M., McGuire, A. D., Norby, R. J., Roy Chowdhury, T., Richter, A., Santruckova, H., Schädel, C., Schuur, E. A. G., Sloan, V. L., Turetsky, M. R. and Waldrop, M. P.: A pan-Arctic synthesis of CH₄ and CO₂ production from anoxic soil incubations, *Glob. Chang. Biol.*, 21, 2787–2803, 2015.
- 1015 Treat, C. C., Bloom, A. A. and Marushchak, M. E.: Nongrowing season methane emissions—a significant component of annual emissions across northern ecosystems, *Glob. Chang. Biol.*, 24, 3331–3343, 2018.
- Walz, J., Knoblauch, C., Böhme, L. and Pfeiffer, E. M.: Regulation of soil organic matter decomposition in permafrost-affected Siberian tundra soils - Impact of oxygen availability, freezing and thawing, temperature, and labile organic matter, *Soil Biol. Biochem.*, 110, 34–43, 2017.
- 1020 Wania, R., Ross, I. and Prentice, I. C.: Integrating peatlands and permafrost into a dynamic global vegetation model: 1. Evaluation and sensitivity of physical land surface processes, *Global Biogeochem. Cycles*, 23, GB3014, 2009.
- Wania, R., Ross, I. and Prentice, I. C.: Implementation and evaluation of a new methane model within a dynamic global vegetation model: LPJ-WHyMe v1.3.1, *Geosci. Model Dev.*, 3, 565–584, 2010.
- 1025 Wania, R., Melton, J. R., Hodson, E. L., Poulter, B., Ringeval, B., Spahni, R., Bohn, T., Avis, C. A., Chen, G., Eliseev, A. V., Hopcroft, P. O., Riley, W. J., Subin, Z. M., Tian, H., Van Bodegom, P. M., Kleinen, T., Yu, Z. C., Singarayer, J. S., Zürcher, S., Lettenmaier, D. P., Beerling, D. J., Denisov, S. N., Prigent, C., Papa, F. and Kaplan, J. O.: Present state of global wetland extent and wetland methane modelling: methodology of a model inter-comparison project (WETCHIMP), *Geosci. Model Dev.*, 6, 617–641, 2013.
- 1030 Weaver, A. J., Eby, M., Wiebe, E. C., Bitz, C. M., Duffy, P. B., Ewen, T. L., Fanning, A. F., Holland, M. M., MacFayden, A., Matthews, H. D., Meissner, K. J., Saenko, O., Schmittner, A., Wang, H. and Yoshimori, M.: The UVic Earth System Climate Model: Model description, climatology, and applications to past, present and future climates, *Atmosphere-Ocean*, 39, 361–428, 2001.
- Whalen, S. C.: Biogeochemistry of methane exchange between natural wetlands and the atmosphere, *Environ. Eng. Sci.*, 22, 73–94, 2005.
- 1035 Wheeler, B. D.: Water and plants in freshwater wetlands, in *Eco-Hydrology*, edited by A. J. Baird and R. L. Wilby, pp. 127–180, Routledge, London., 1999.
- Whiticar, M. J. and Faber, E.: Methane oxidation in sediment and water column environments—Isotope evidence, *Adv. Org. Geochemistry*, 10, 759–768, 1985.
- 1040 Wild, B., Gentsch, N., Čapek, P., Diáková, K., Alves, R. J. E., Bárta, J., Gittel, A., Hugelius, G., Knoltsch, A., Kuhry, P., Lashchinskiy, N., Mikutta, R., Palmtag, J., Schleper, C., Schneckner, J., Shibistova, O., Takriti, M., Torsvik, V. L., Urlich, T., Watzka, M., Šantrůčková, H., Guggenberger, G. and Richter, A.: Plant-derived compounds stimulate the decomposition of organic matter in arctic permafrost soils, *Sci. Rep.*, 6, 25607, 2016.
- Wu, Y., Versegny, D. and Melton, J.: Integrating peatlands into the coupled Canadian Land Surface Scheme (CLASS) v3.6 and the Canadian Terrestrial Ecosystem Model (CTEM) v2.0, *Geosci. Model Dev.*, 9, 2639–2663, 2016.
- 1045 Xu, X., Elias, D. A., Graham, D. E., Phelps, T. J., Carroll, S. L., Wullschlegel, S. D. and Thornton, P. E.: A microbial functional group-based module for simulating methane production and consumption: Application to an incubated permafrost soil, *J. Geophys. Res. G Biogeosciences*, 120, 1315–1333, 2015.



- 1050 Xu, X., Yuan, F., Hanson, P. J., Wullschleger, S. D., Thornton, P. E., Riley, W. J., Song, X., Graham, D. E., Song, C. and Tian, H.: Reviews and syntheses: Four decades of modeling methane cycling in terrestrial ecosystems, *Biogeosciences*, 13, 3735–3755, 2016.
- Yvon-Durocher, G., Allen, A. P., Bastviken, D., Conrad, R., Gudas, C., St-Pierre, A., Thanh-Duc, N. and Del Giorgio, P. A.: Methane fluxes show consistent temperature dependence across microbial to ecosystem scales, *Nature*, 507, 488–491, 2014.
- 1055 Zalman, C. A., Meade, N., Chanton, J., Kostka, J. E., Bridgham, S. D. and Keller, J. K.: Methylotrophic methanogenesis in sphagnum-dominated peatland soils, *Soil Biol. Biochem.*, 118, 156–160, 2018.
- Zhang, B., Tian, H., Lu, C., Chen, G., Pan, S., Anderson, C. and Poulter, B.: Methane emissions from global wetlands: An assessment of the uncertainty associated with various wetland extent data sets, *Atmos. Environ.*, 165, 310–321, 2017a.
- 1060 Zhang, Z., Zimmermann, N. E., Stenke, A., Li, X., Hodson, E. L., Zhu, G., Huang, C. and Poulter, B.: Emerging role of wetland methane emissions in driving 21st century climate change, *Proc. Natl. Acad. Sci. U. S. A.*, 114, 9647–9652, 2017b.
- Zhang, Z., Zimmermann, N. E., Calle, L., Hurtt, G., Chatterjee, A. and Poulter, B.: Enhanced response of global wetland methane emissions to the 2015-2016 El Niño-Southern Oscillation event, *Environ. Res. Lett.*, 13, 074009, 2018.
- 1065 Zhu, Q., Peng, C., Chen, H., Fang, X., Liu, J., Jiang, H., Yang, Y. and Yang, G.: Estimating global natural wetland methane emissions using process modelling: spatio-temporal patterns and contributions to atmospheric methane fluctuations, *Glob. Ecol. Biogeogr.*, 24, 959–972, 2015.
- Zickfeld, K., Eby, M., Matthews, H. D. and Weaver, A. J.: Setting cumulative emissions targets to reduce the risk of dangerous climate change, *Proc. Natl. Acad. Sci. U. S. A.*, 106, 16129–16134, 2009.
- 1070 Zona, D., Gioli, B., Commane, R., Lindaas, J., Wofsy, S. C., Miller, C. E., Dinardo, S. J., Dengel, S., Sweeney, C., Karion, A., Chang, R. Y.-W., Henderson, J. M., Murphy, P. C., Goodrich, J. P., Moreaux, V., Liljedahl, A., Watts, J. D., Kimball, J. S., Lipson, D. A. and Oechel, W. C.: Cold season emissions dominate the Arctic tundra methane budget, *Proc. Natl. Acad. Sci. U. S. A.*, 113, 40–45, 2016.